Sestrin is a key regulator of stem cell function and lifespan in response to dietary amino acids

Jiongming Lu[1], Ulrike Temp[1], Andrea Müller-Hartmann[1], Jacqueline Esser[1], Sebastian Grönke[1,*], Linda Partridge[1,2,*]

[*]Corresponding author

Affiliations

1. Max Planck Institute for Biology of Ageing, Köln 50931, Germany.

2. Institute of Healthy Ageing, and Department of Genetics, Evolution and Environment, University College London, London WC1E 6BT, UK.

Corresponding contact details:

Sebastian Grönke: sebastian.groenke@age.mpg.de

Linda Partridge: linda.partridge@age.mpg.de

Abstract

Dietary restriction (DR) promotes healthy ageing in diverse species. Essential amino acids play a key role, but the molecular mechanisms are unknown. The evolutionarily conserved Sestrin protein, an inhibitor of activity of the TORC1 complex, has recently been discovered as a sensor of amino acids *in vitro*. Here we show that *Sestrin* null mutant flies have a blunted response of lifespan to DR. A mutant *Sestrin* fly line, with blocked amino acid binding and TORC1 activation, showed delayed development, reduced fecundity, extended lifespan and protection against lifespan-shortening, high protein diets. Sestrin mediated reduced intestinal stem cell activity and gut cell turnover from DR, and stem cell proliferation in response to dietary amino acids, by regulating the TOR pathway and autophagy. Sestrin expression in intestinal stem cells was sufficient to maintain gut homeostasis and extend lifespan. Sestrin is thus a molecular link between dietary amino acids, stem cell function and longevity.

Introduction

Dietary restriction (DR) can extend lifespan in diverse species, including fruit flies and rodents[1,2]. DR not only increases longevity, but also induces broad health improvements during ageing in rodents, primates and humans[3-6]. Restriction of specific dietary components, especially protein, is more important than the overall reduction in calories in producing the responses to DR[7-11]. Furthermore, restriction of specific essential amino acids including methionine[12,13] and the branched chain amino acids (BCAAs) leucine, isoleucine and valine[14-16] can extend lifespan. However, the underlying molecular and cellular mechanisms are still elusive.

DR maintains the health of multiple tissues, including brain, bone, muscle, gut and fat[17-19]. However, their contributions to DR-mediated longevity are currently unclear. In *Drosophila* the gut is a key mediator[20]. This tissue consists of self-renewable intestinal stem cells (ISCs), transient enteroblasts, and differentiated absorptive enterocytes and enteroendocrine cells[21,22]. Interestingly, both ISCs and enterocytes contribute to fly longevity[23,24]. Furthermore, both the geroprotective TORC1 inhibitor rapamycin[25] and amino acid restriction[14] improve gut health. However, the molecular mechanisms at work are currently unknown.

Reduced activity of the nutrient sensing insulin/IGF-1/TOR (IIT) network can extend lifespan across model organisms[1,2], and it plays a key role in the responses to DR, with the longevity of flies with reduced IIT signaling unresponsive to DR[11,26,27]. The IIT network monitors and integrates different environmental cues including amino acids[28,29], which mainly affect the TOR branch of the network. Recently, Sestrin

proteins have been shown to act as upstream negative regulators of TORC1 activity *in vitro* in response to amino acid availability[30]. Sestrins are highly conserved proteins that are induced in cells under environmental challenges, including oxidative stress, DNA damage, and amino acid starvation[31]. Mammalian genomes encode three Sestrin proteins, while the *Drosophila* genome encodes a single Sestrin orthologue. Sestrin proteins inhibit TORC1 activity, both through activation of the adenosine monophosphate (AMP)-activated protein kinase (AMPK), and through interaction with the GATOR complex[30,32]. Sestrin directly binds to amino acids, resulting in the dissociation of the Sestrin-GATOR2 complex and increased TORC1 activity[33,34]. Based on these *in vitro* studies, Sestrin has been postulated to act as a leucine sensor[33,34]. However, whether Sestrin performs similar functions *in vivo* is not known[35]. In *Drosophila*, loss of *Sestrin* causes age-associated pathologies, probably through chronic TORC1 activation and hence reduced autophagy[36]. Surprisingly, however, *Sestrin* mutants were reported to have normal lifespan[31]. Thus, the *in vivo* roles of Sestrin remain to be determined.

In this study, we uncovered roles of amino acid sensing by Sestrin in whole organism physiology *in vivo.* Loss of *Sestrin* blunted the normal increase in lifespan in response to DR. We identified a key role of Arg407 in the fly Sestrin protein for amino acid binding *in vitro*. We generated a *Sestrin* mutant fly line ($Sesn^{R407A}$) in which amino acid binding to the endogenous Sestrin protein was blocked, which prevented activation of TORC1 by amino acids *in vivo*. $Sesn^{R407A}$ mutant flies showed reduced TORC1 activity, decreased growth, delayed development, increased lifespan and improved gut homeostasis. Adding back amino acids to DR food medium increased ISC proliferation in control flies, but this effect was blocked in $Sesn^{R407A}$ mutant flies. Sestrin regulated

lifespan and ISC maintenance via the TOR pathway, and autophagy in ISCs was essential to regulate gut cell turnover. Furthermore, Sestrin expression in ISCs was sufficient to maintain gut homeostasis and increase fly lifespan, establishing Sestrin as a novel molecular link that regulates stem cell proliferation, intestinal health and longevity in response to dietary amino acids.

Results

Absence of Sestrin attenuates the response of lifespan to dietary restriction

To determine the role of Sestrin in amino acid sensing *in vivo*, we used a previously generated *Sestrin* mutant allele[36], termed $Sesn^{3F6}$, in which the first two exons of the *Sestrin* gene are deleted (Extended Data Fig. 1a). $Sesn^{3F6}$ mutant flies had greatly reduced *Sestrin* mRNA levels and no detectable Sestrin protein (Extended Data Fig. 1b,c), suggesting it to be a strong hypomorph or even a functionally null allele. The $Sesn^{3F6}$ allele was backcrossed into the *white Dahomey* (w^{Dah}) wild type strain and w^{Dah} flies were used as controls in subsequent experiments. We examined the effect of loss of *Sestrin* on whole organism physiology by measuring development time. $Sesn^{3F6}$ mutant flies were viable and had more rapid egg-to-adult development and slightly increased body weight compared with controls (Extended Data Fig. 1d,e), consistent with increased TORC1 activity during larval development, as previously reported[36]. Loss of *Sestrin* therefore increased larval growth rate and adult body size.

We next assessed the *in vivo* role of Sestrin in the adult fly. In *Drosophila*, increased lifespan from DR is mediated almost exclusively by restriction of essential amino acids in the diet[11]. We therefore measured the response of lifespan to DR in $Sesn^{3F6}$ mutant flies. In *Drosophila* DR can be achieved by diluting the yeast component of the diet, and we measured survival of female flies on four different food dilutions: 0.1x, 0.5x, 1.0x and 2.0x the yeast content of the normal fly diet. w^{Dah} females showed a typical tent-shaped response of lifespan to DR, with the longest median lifespan on the 0.5x and 1.0x yeast foods (Fig. 1a,b). Interestingly, $Sesn^{3F6}$ mutant flies showed an attenuated increase in lifespan at these two yeast concentrations, with median lifespan

compared with controls reduced by 11% and 13% on the 0.5x and 1.0x yeast food, respectively (Fig. 1a,b). However, the mutants had similar lifespan to controls at high and low yeast concentrations, showing that they were normally viable and that their attenuated lifespan was specific to DR conditions. Cox proportional hazard (CPH) analysis confirmed that the interaction between genotype and treatment was significant ($P < 0.0001$), demonstrating that *Sesn*^{3F6} mutant flies responded to the DR treatment differently from controls. Thus, in *Drosophila*, although parallel systems also mediate the response, Sestrin function is essential to achieve full lifespan extension in response to DR.

Generation of an amino acid sensing defective *Sestrin* fly mutant

Sestrin activity towards TORC1 *in vitro* is directly regulated by its binding of amino acids[33]. To determine if the amino acid sensing ability of Sestrin is important for its function *in vivo*, we generated a novel fly strain in which the putative amino acid binding pocket of the *Drosophila* Sestrin protein was mutated. In the human Sestrin2 protein Arginine residue 390 (R390) is an essential component of the binding pocket, and mutation of R390 to alanine completely abolishes leucine binding[34]. By sequence homology analysis we identified arginine 407 (R407) as the corresponding residue in the *Drosophila* Sestrin protein (Fig. 2a). Modeling the structure of the *Drosophila* Sestrin based on the structure of the human protein showed that R407 is indeed located in a pocket-like structure (Fig. 2b), suggesting that R407 might be a key residue for amino acid binding in the fly Sestrin protein. In order to test this, we performed Sestrin-GATOR2 interaction assays *in vitro*[33] (Fig. 2c,d). An HA-tagged *Drosophila* Sestrin wild type or R407A mutant protein was co-expressed with the fly Flag-WDR24 in HEK-293T cells. Individual amino acids were added to the cell lysate followed by Flag

immunoprecipitation of the WDR24 protein. Addition of leucine, isoleucine, valine and methionine interfered with the Sestrin-GATOR2 interaction of the wild type Sestrin protein, but they did not affect the interaction of the Sestrin R407A mutant protein (Fig. 2c,d). The R407 residue thus plays a key role in the amino acid binding of the *Drosophila* Sestrin protein. To analyze the *in vivo* impact of amino acid sensing by Sestrin on fly physiology, we employed CRISPR-Cas9 to introduce the R407A mutation into the endogenous *Sestrin* gene locus (Fig. 2e). In addition, we introduced a Myc tag before the TGA stop codon of the *Sestrin* gene to allow easy detection of the protein by immunoblotting, and the resulting fly line was termed $Sesn^{R407A}$. To control for the presence of the Myc tag, we generated an additional fly strain termed $Sesn^{wt}$, which only contained the Myc tag. We next used qRT-PCR and immunoblotting analysis to show that the introduced $Sesn^{R407A}$ mutation did not affect *Sestrin* mRNA or protein levels, respectively (Extended Data Fig. 2a-c).

To investigate how the Sestrin R407A mutation affected amino acid sensing by the TORC1 pathway in flies, we made amino acid starvation and stimulation experiments using the fat body of *Drosophila* larvae, because it responds rapidly to changes in nutrient availability, including of amino acids[37,38]. When larval fat bodies were deprived of amino acids, phosphorylation of S6 kinase (S6K), a direct downstream target of TORC1, was low and did not differ between $Sesn^{wt}$ and $Sesn^{R407A}$ mutants (Fig. 2f,g). We first measured the response of pre-starved larval fat body tissue to leucine stimulation, which resulted in a ~3-fold increase in pS6K levels in $Sesn^{wt}$ controls (Fig. 2f,g). In contrast, there was no increase in pS6K levels in fat bodies of $Sesn^{R407A}$ mutants (Fig. 2f,g). The $Sesn^{R407A}$ mutation therefore interfered with leucine-mediated activation of TORC1. We next asked whether the $Sesn^{R407A}$ mutation would also block the

activation of TORC1 signaling by all amino acids together. In *Sesn*^{wt} flies we observed a much greater ~10-fold increase in pS6K levels upon stimulation with all amino acids than with leucine treatment alone (Fig. 2h,i). One or more amino acids in addition to leucine are therefore required for full activation of TORC1 activity in the larval fat body. Interestingly, the increase in TORC1 activity in response to stimulation by all amino acids was almost completely blocked in *Sesn*^{R407A} mutants (Fig. 2h,i). This suggests that the *Sesn*^{R407A} mutation blocks not only leucine-mediated TORC1 stimulation, but also stimulation by other amino acids, consistent with the finding that isoleucine, valine and methionine were also able to interrupt Sestrin-GATOR2 interaction (Fig. 2c,d). The result also indicates that the inhibitory effect of the amino acid insensitive Sestrin R407A protein on TORC1 activity cannot be compensated by other amino acid sensing mechanisms.

We next addressed whether the *Sesn*^{R407A} mutation also affected TORC1 activity under physiological conditions. Immunoblotting analysis on fat bodies of 3rd instar larvae growing on normal fly food showed that pS6K levels were reduced by ~60% in *Sesn*^{R407A} mutants compared with *Sesn*^{wt} controls (Fig. 3a,b), indicating chronically reduced activity of TORC1 in *Sesn*^{R407A} mutant larvae. We also tested whether the *Sesn*^{R407A} mutation affected activity of the TORC2 complex, by measuring phosphorylation of AKT at serine residue 505 (Ser505). Ser505 pAKT levels did not differ between *Sesn*^{R407A} mutant and *Sesn*^{wt} controls (Fig. 3a,c), demonstrating that the *Sesn*^{R407A} mutation affected only activity of the TORC1 complex. Finally, we measured threonine 184 phosphorylation of AMPKα, another downstream target of Sestrin, and found that it did not differ between *Sesn*^{R407A} mutant and *Sesn*^{wt} control larvae (Extended Data Fig. 3a,b). The amino acid sensing defective Sestrin R407A mutant protein

therefore specifically down-regulated TORC1 activity, and not activity of the TORC2 complex or of AMPK.

To further characterize the physiological consequences of the Sestrin R407A mutation *in vivo*, we measured development time and female fecundity of $Sesn^{R407A}$ mutants, because both traits depend on amino acid availability. $Sesn^{R407A}$ mutant flies were fully viable but had a significantly delayed development (Fig. 3d) and reduced adult body weight (Fig. 3e) in comparison to $Sesn^{wt}$ controls. To test whether these growth effects were cell autonomous, we used the *FLP/FRT* system to generate mosaic clones in the larval fat body. Cells homozygous for the $Sesn^{R407A}$ mutation were significantly smaller than wild type cells (Extended Data Fig. 3c,d), demonstrating that the mutant $Sestrin^{R407A}$ protein reduced cell growth in a cell autonomous manner. $Sesn^{R407A}$ mutant females also showed a 30% decreased cumulative egg production, mainly caused by reduced fecundity early in life (Extended Data Fig. 3e,f). Amino acid insensitive $Sesn^{R407A}$ mutants therefore had delayed development, reduced growth and fecundity, consistent with chronically reduced TORC1 activity.

The amino acid insensitive $Sesn^{R407A}$ mutation blunts the shortening of lifespan on a high protein diet

To test the role of amino acid sensing by Sestrin in the response to DR, we measured the lifespan of $Sesn^{R407A}$ mutant flies under DR conditions. $Sesn^{R407A}$ mutants showed only a small survival advantage on the 0.5x and 1.0x DR food, with a median lifespan increase of 11% and 14%, respectively. In contrast, median lifespan was increased by 40% on the high yeast diet (2.0x SYA), mainly due to a greater decrease in survival of control flies on this diet (Fig. 3f,g). CPH analysis revealed that the interaction between

genotype and diet treatment was significant ($P < 0.0001$), confirming that $Sesn^{R407A}$ flies responded significantly differently from $Sesn^{wt}$ flies to DR. The $Sesn^{R407A}$ mutation hence increased lifespan under non-starvation conditions and attenuated the negative effect of high dietary yeast on lifespan, which is therefore partially mediated through amino acid sensing by Sestrin.

Sestrin function is important for maintenance of intestinal stem cells and gut health by DR

We next addressed in which tissue Sestrin function is required to modulate the response of lifespan to DR. The fly gut has recently been identified as a key tissue for the organismal response to DR[20,39]. Maintenance of gut homeostasis largely relies on stem cell mediated renewal of absorptive enterocytes[23,40] and preservation of stem cell activity has been associated with increased survival in flies[23]. Since there are no transient-amplifying cells in the adult fly gut, the mitotic marker phospho-Histone 3 (pH3) directly reflects the activity of stem cells[21,22]. We measured the number of pH3-positive cells in guts of $Sesn^{3F6}$ loss-of-function mutants and w^{Dah} control females under fully fed (2.0x) and DR (1.0x) conditions. Consistent with previous studies[20], DR decreased stem cell activity in the gut of control flies, with a reduction of ~50% in pH3-positive cells per gut (Fig. 4a,b). In contrast, DR did not decrease stem cell activity in the gut of $Sesn^{3F6}$ mutant flies, with no difference from the number of pH3-positive cells in guts of w^{Dah} controls on 2.0x food (Fig. 4a,b). pH3 staining provides a snap shot of stem cell activity at a given time point. To measure gut cell turnover rates directly, we used the esg^{ts} *F/O* system, which marks stem cells and all their progeny by heat shock-induced expression of a GFP protein. GFP-marked regions indicate newly generated cells, and their area, when compared with the corresponding total gut area,

indicates gut cell turnover rates. In line with the results from pH3 staining, w^{Dah} control flies showed a ~40% decrease in gut turnover rates under DR conditions (Fig. 4c,d). In contrast, we found no difference in gut cell turnover rates when *Sestrin* was knocked down specifically in ISCs using RNAi (Fig. 4c,d). Sestrin function in ISCs is hence essential for reduced cell turnover and stem cell maintenance under DR conditions.

We next measured stem cell activity in the amino-acid-insensitive $Sesn^{R407A}$ mutant flies. Consistent with w^{Dah} control flies, $Sesn^{wt}$ control flies had high levels of intestinal pH3-positive cells under fully fed conditions and reduced levels under DR conditions (Fig. 4e,f). In contrast, $Sesn^{R407A}$ mutants showed strongly decreased ISC activity under full feeding, and DR did not further reduce the number of pH3-positive cells (Fig. 4e,f). Consistently, gut cell turnover rates were also low in $Sesn^{R407A}$ mutants on the 2.0x diet and were not further decreased by DR (Fig. 4g,h). To test whether dietary amino acid restriction was causal in reduced gut cell turnover under DR conditions, we added back amino acids to the 1.0x DR food and measured intestinal cell turnover rates. Addition of all amino acids to the 1.0x DR diet increased gut cell turnover rates of $Sesn^{wt}$ control flies to a similar level to that observed on the 2.0x fully fed diet (Fig. 4i). Importantly, gut cell turnover rates of $Sesn^{R407A}$ mutant flies were not affected by addition of amino acids (Fig. 4i). Furthermore, addition of leucine, isoleucine, valine and methionine, the four amino acids involved in the regulation of Sestrin activity, to the DR medium was sufficient to increase gut turnover rates in $Sesn^{wt}$ controls but not in $Sesn^{R407A}$ mutants (Fig. 4j). Sensing of these amino acids by Sestrin in ISCs or their progeny cells hence regulates stem cell activity in response to changes in dietary amino acids. Improved intestinal stem cell homeostasis is associated with a healthier gut[20]. Thus, in order to address the role of Sestrin in maintenance of gut health under DR we measured gut

pathology in old flies using a dysplasia assay[14,20] and epithelial barrier function using a Smurf assay[41]. In control flies, DR reduced age-related gut dysplasia and the proportion of flies with a Smurf phenotype (Extended Data Fig. 4a-f). In contrast, dysplasia and incidence of Smurfs of $Sesn^{3F6}$ loss-of-function mutant flies was not improved by DR, while $Sesn^{R407A}$ mutant flies showed lower incidence of both phenotypes that could not be further reduced by the DR treatment (Extended Data Fig. 4a-f). Thus, these results illustrate that Sestrin is an important regulator of gut health in response to dietary protein restriction.

Sestrin acts in ISCs to maintain stem cell function and gut health

To identify the cell types in which Sestrin acts to maintain gut health, we employed cell-type-specific over-expression of *Sestrin*. First, we measured ISC activity upon ubiquitous over-expression of *Sestrin* using the inducible *daGS* Gene-Switch driver in young (day 10), middle-aged (day 30) and old (day 50) flies (Fig. 5a,b). Consistent with a previous report[23], we observed an increase of pH3-positive cells during ageing under non-induced conditions (Fig. 5b). *Sestrin* over-expression had only a small effect on stem cell activity in young flies, but prevented the age-related increase. Generalized linear modeling (GLM) indicated that stem cell activity increased significantly less with age when *Sestrin* expression was induced ($P < 0.05$). Ubiquitous *Sestrin* over-expression was thus sufficient to preserve proliferative capacity of ISCs during ageing. To determine which cell type underlay this effect, we measured pH3-positive cell numbers in middle-aged and old flies, where we observed strongest effects. We used the *5966GS* driver[24] to over-express *Sestrin* specifically in absorptive enterocytes, and did not observe reduced stem cell activity (Fig. 5c). In contrast, induction of *Sestrin* expression specifically in stem cells by using the *5961GS* driver[23] led to a clear

reduction in stem cell activity (Fig. 5d). These results together imply that the function of Sestrin in ISCs, but not in enterocytes, is important for its role in stem cell maintenance.

To address how Sestrin affects stem cell function we first measured their cell cycle state upon *Sestrin* over-expression using the Fly-Fucci system, which relies on fluorochrome-tagged proteins to distinguish G1, S, and G2 of the cell cycle. *Sestrin* over-expression in ISCs increased the proportion of cells in the G1 phase (Fig. 5e). Additionally, a prolonged G1 phase indicates an inhibition of G1-S transition, a phenotype known to be caused by reduced TORC1 activity[42]. To further test whether Sestrin function in ISCs was also causal for the improved gut health, we performed gut dysplasia and Smurf assays. We found that *Sestrin* over-expression reduced gut dysplasia (Fig. 5f,g) and improved gut barrier function (Fig. 5h). These results demonstrate that ISC-specific Sestrin expression improves gut homeostasis.

Sestrin regulates lifespan and intestinal stem cell maintenance via the TOR pathway

Sestrin has been identified as an amino acid sensor upstream of TORC1[33]. To test whether the lifespan and stem cell phenotypes we observed in *Sestrin* mutants were indeed caused by regulation of the TOR pathway, we used the drug rapamycin to specifically inhibit TOR in *Sestrin* mutant flies. If Sestrin works exclusively via the TOR pathway, rapamycin treatment should revert the detrimental phenotypes caused by loss of *Sestrin* function and should not cause additive effects when combined with the amino acid insensitive $Sesn^{R407A}$ mutation. Consistent with this hypothesis, rapamycin treatment increased lifespan of $Sesn^{3F6}$ mutant flies and, while $Sesn^{3F6}$

mutant flies were short-lived compared with controls in the absence of the drug, there was no difference in lifespan compared with wild type control flies on the rapamycin diet (Fig. 6a). Furthermore, rapamycin treatment did not extend lifespan of the already long-lived $Sesn^{R407A}$ mutant flies (Fig. 6b), suggesting that Sestrin acts upstream of the TOR pathway to affect lifespan. We next investigated whether the same hypothesis also holds true for the ISC phenotypes. Rapamycin treatment reduced the increased ISC activity of $Sesn^{3F6}$ loss-of-function mutant flies and there was no difference between wild type controls and $Sesn^{R407A}$ mutants upon rapamycin treatment (Fig. 6c-f). Furthermore, rapamycin treatment blocked the increase in gut cell turnover upon knockdown of *Sestrin* in ISCs, and there were no additive effects on gut cell turnover rate when rapamycin was fed to flies over-expressing *Sestrin* in these cells (Fig. 6g-j and Extended Data Fig. 5a,b). Taken together, these results suggest that Sestrin regulates lifespan and ISC activity via the TOR pathway.

Sestrin increases autophagy in ISCs to regulate gut cell turnover

Autophagy is a key downstream mediator of the TORC1 pathway[43], and increased autophagy is essential for rapamycin-mediated longevity in *Drosophila*[27]. To investigate whether Sestrin regulates autophagy in ISCs, we used a fluorescence tagged Atg8a reporter, *UAS-mCherry::Atg8a*, as a read-out for levels of autophagy. The *esg-Gal4* driver was used to express this reporter in ISCs, and GFP was co-expressed to mark these cells. mCherry-positive cells were counted and the ratio to total GFP cells was calculated. A low basal level of autophagy was detected in wild-type stem cells. Interestingly, a significant increase of ~3-fold was detected when *Sestrin* was over-expressed (Fig. 7a,b). We next clarified whether the accumulation of the mCherry signal was indeed due to induced autophagy, or instead attributable to a block of

autophagic flux, by using the *UAS-GFP::mCherry::Atg8a* reporter[44,45]. When this reporter was co-expressed with *Sestrin*, the dominant signal we detected was mCherry (Extended Data Fig. 5c), indicating that autophagic flux was not impaired. These results suggest that Sestrin induces autophagy in ISCs, probably by inhibiting TORC1 activity. We next addressed whether the increase in autophagy was functionally relevant for gut cell turnover. Therefore, we first over-expressed *Atg1*, a key upstream regulator of autophagy[43], in ISCs and measured gut cell turnover rates. Over-expression of *Atg1* reduced gut cell turnover rates (Fig. 7c,d), suggesting that induction of autophagy is sufficient to block gut turnover. Next we blocked autophagy in ISCs by knocking down *Atg5* via RNAi[46]. *Atg5* knockdown did not have an effect on gut cell turnover in the wild type background, but it blocked the effect of *Sestrin* over-expression on gut cell turnover (Fig. 7c,d). Taken together these results identify increased autophagy in ISCs as an essential downstream mechanism by which Sestrin regulates gut physiology.

Sestrin over-expression in intestinal stem cells extends lifespan

Improved ISC maintenance has been associated with increased organismal survival in flies[23]. Thus, we next addressed whether ISC-specific over-expression of *Sestrin* would be sufficient to increase adult survival. We first measured survival of adult flies in which *Sestrin* was ubiquitously over-expressed under the control of the *daGS* driver, which significantly increased lifespan, with a median extension of 10% (Fig. 8a). Over-expression of *Sestrin* in neurons or fat bodies using the *elavGS* and *S$_1$106GS* drivers, respectively, did not cause lifespan extension (Fig. 8b,c), and nor did over-expression using the enterocyte specific *5966GS* driver (Fig. 8d). In contrast, over-expression of *Sestrin* under the control of the ISC-specific *5961GS* driver resulted in a significant lifespan extension, again with a median lifespan extension of ~10% (Fig. 8e). Relative

lifespan extension was even greater on a high yeast diet (2.0x SYA), with an 15% increase in median lifespan (Fig. 8f), suggesting that Sestrin function in stem cells protects against the lifespan shortening effects of a protein rich diet. Thus, *Sestrin* over-expression in ISCs could extend fly lifespan to the same extent as ubiquitous over-expression, suggesting that ISCs are a key cell type mediating the effects of *Sestrin* gain-of-function on survival.

In summary, our study identified the evolutionarily conserved Sestrin protein as a key regulator of stem cell activity under DR in *Drosophila*. Sestrin regulates TORC1 signaling and proliferation of ISCs in response to the availability of dietary amino acids. Therefore, our data establish Sestrin as a novel molecular link that mediates the effects of dietary amino acid restriction on ISC function and health and on organismal lifespan.

Discussion

Dietary restriction is to date the most effective intervention to lengthen life and healthspan in animals and short-term dietary interventions can also improve health in humans[47]. However, in humans long-term compliance greatly limits its applicability to the wider population. Understanding the molecular mechanisms underlying the beneficial effects of DR could lead to development of novel treatments based on DR mimetics. Here, we identified the evolutionarily conserved amino acid sensor protein Sestrin as a key regulator of stem cell function, intestinal health and survival in response to dietary amino acids. Thus, our findings implicate Sestrin as a novel target for anti-ageing interventions.

Sestrin has been identified as an amino acid sensing protein that acts as a negative regulator of TORC1 activity via the GATOR/Rag complex[33,34]. This role of Sestrin has mainly been studied in the context of acute amino acid stimulation of previously amino acid starved cultured cells, and the *in vivo* relevance of Sestrin in amino acid sensing is still under debate[35]. Although it binds to several essential amino acids *in vitro*, in mammals Sestrin has been postulated to act mainly as a leucine sensor[33,34]. We found that leucine addition only resulted in a 3-fold increase in pS6K levels, a proxy for TORC1 activity, while addition of all amino acids induced a 10-fold increase in larval fat bodies. This result is notable given that leucine was supplied at a 20-fold higher concentration as compared to the addition of all amino acids. Thus, a combination of several amino acids is needed for full activation of TORC1 signaling in the *Drosophila* fat body. Importantly, leucine-induced TORC1 activation was completely dependent on Sestrin, implying that there are no other mechanisms leading to leucine sensing by

TORC1. TORC1 activation by all amino acids was also strongly reduced in amino acid insensitive *Sesn*^{R407A} mutants, confirming that other amino acids in addition to leucine are required for full activation of TORC1 activity by Sestrin. In summary, our results indicate that *in vivo* Sestrin senses not only leucine but also the other branched chain amino acids and methionine.

Sestrin has been previously studied in both flies[36] and mice[48-50], although not in the context of dietary amino acid sensing. *Sestrin* mutant flies exhibit a broad range of age-associated pathologies[36] but, surprisingly, were not short-lived[31]. Our findings indicate that longevity of *Sestrin* mutants is dependent on the nutritional context, with mutant flies short-lived compared to controls specifically under DR conditions, but not on a high protein diet. This is consistent with the chronically increased activity of the TORC1 pathway in *Sestrin* mutant flies[36], which is expected to have a bigger detrimental effect under DR conditions than on a high protein diet, where TOR activity is already high.

Reduced TOR signaling is an important downstream mediator of DR benefits[27,51]. Lowered dietary amino acids have been shown to be causal for DR-induced longevity in flies[11], but the molecular mechanisms mediating these benefits and the tissues they act in are still elusive. Our results establish Sestrin as an important mediator of DR benefits, however, loss of *Sestrin* did not fully block the beneficial effects of DR on longevity and the combination of DR and the *Sesn*^{R407A} mutation resulted in a greater extension of lifespan than each treatment individually, indicating that DR and TOR might also work via independent mechanisms. This hypothesis is consistent with recent

gene expression studies in flies and mammals, which suggest both shared and independent mechanisms of DR and reduced TOR signaling[52-54].

The gut is a key tissue mediating health benefits of DR and reduced TOR signaling[20,25,55,56]. Importantly, we showed that restriction of dietary amino acids is causal for improved gut homeostasis under DR. Consistent with the binding affinity of Sestrin *in vitro*, BCAAs and methionine seem to play a causal role in this context. Concordantly, restriction of BCAAs has recently been shown to be sufficient to improve gut homeostasis in flies[14]. Noteworthy, also restriction of three non BCAA caused improved gut homeostasis[14], which suggest the involvement of additional amino acid sensitive mechanisms in addition to Sestrin. The Tuberous sclerosis complex 2 (TSC2) protein is implicated in amino-acid-dependent regulation of TORC1[57], and the TSC1/2 complex regulates ISC maintenance in flies via the TORC1 pathway[58-60]. Thus, Sestrin and TSC2 might act in concert or in parallel in regulating amino-acid-dependent regulation of stem cell maintenance. Interestingly, the $Sesn^{R407A}$ mutation blocked gut turnover rates also upon supplementation of all amino acids, which suggests that strong *Sestrin* gain-of-function in ISCs can override the input of other amino acid sensing systems.

DR and the TOR pathway also play important roles in maintenance of adult stem cells in mammals[61-63]. The effect of DR on stem cell maintenance can be indirect, via TORC1 signaling in stem cell niche cells, or via regulation of TORC1 directly in stem cells. For example, DR caused down-regulation of TORC1 activity in the radioresistant, reserve ISC pool, which contributes to enhanced tissue regeneration after DR[64]. Importantly, leucine supplementation was sufficient to induce TORC1 activity in reserve ISCs[64],

implicating amino acid sensing systems in TORC1-mediated regulation of ISC maintenance in mammals. However, whether the mammalian Sestrin homologues are involved in this regulation is currently unknown.

We show that Sestrin regulates lifespan via the TOR pathway and established autophagy as an essential mediator downstream of TOR that regulates gut cell turnover. Autophagy is required for stem cell maintenance and intestinal homeostasis in flies[65] and mammals[66,67], however whether upregulation of autophagy in ISCs is sufficient to extend lifespan is currently unknown. Additional mechanisms downstream of TORC1, like inhibition of S6K[27] and of RNA Pol III[68] have also been implicated in ISC maintenance and longevity, and therefore might also contribute to the effect of Sestrin in ISCs. In summary our results establish Sestrin as a novel molecular link that mediates the effects of dietary amino acid restriction on TORC1 activity in stem cells of the fly gut, thereby maintaining gut health and ensuring longevity.

Acknowledgements

We thank J.H. Lee, B. Edgar, G. Juhasz, the Bloomington Stock Center and the VDRC Stock Center for fly strains and reagents. We are also grateful to all member of the Partridge Lab for helpful insights, and to C. Demetriades for critical comments. Imaging was performed in the FACS & Imaging Core Facility, and amino acid concentrations were determined in the Metabolomics Core Facility at the Max Planck Institute for Biology of Ageing. The work was supported by a SNSF postdoc fellowship (P2BEP3_162093) to J.L. and by funding from the Max Planck Society to L.P.. The research leading to these results has received funding from the European Research Council under the European Union's Seventh Framework Programme (FP7/2007-2013) / ERC grant agreement no. 268739.

Author Contributions

J.L., S.G. and L.P. conceived and designed the study. J.L. conducted most experiments, U.T. and A.M.H provided assistance. J.E. contributed to the generation of transgenic flies. J.L. and S.G. analyzed the data. J.L., S.G. and L.P. wrote the manuscript.

Competing Interests Statement

The authors declare no competing financial interests.

References

1 Fontana, L., Partridge, L. & Longo, V. D. Extending healthy life span--from yeast to humans. *Science* **328**, 321-326, doi:10.1126/science.1172539 (2010).

2 Kenyon, C. J. The genetics of ageing. *Nature* **464**, 504-512, doi:10.1038/nature08980 (2010).

3 Weindruch, R., Walford, R. L., Fligiel, S. & Guthrie, D. The retardation of aging in mice by dietary restriction: longevity, cancer, immunity and lifetime energy intake. *J Nutr* **116**, 641-654, doi:10.1093/jn/116.4.641 (1986).

4 Colman, R. J. *et al.* Caloric restriction delays disease onset and mortality in rhesus monkeys. *Science* **325**, 201-204, doi:10.1126/science.1173635 (2009).

5 Mattison, J. A. *et al.* Impact of caloric restriction on health and survival in rhesus monkeys from the NIA study. *Nature* **489**, 318-321, doi:10.1038/nature11432 (2012).

6 Most, J., Tosti, V., Redman, L. M. & Fontana, L. Calorie restriction in humans: An update. *Ageing Res Rev* **39**, 36-45, doi:10.1016/j.arr.2016.08.005 (2017).

7 Mair, W., Piper, M. D. & Partridge, L. Calories do not explain extension of life span by dietary restriction in Drosophila. *PLoS Biol* **3**, e223, doi:10.1371/journal.pbio.0030223 (2005).

8 Solon-Biet, S. M. *et al.* The ratio of macronutrients, not caloric intake, dictates cardiometabolic health, aging, and longevity in ad libitum-fed mice. *Cell Metab* **19**, 418-430, doi:10.1016/j.cmet.2014.02.009 (2014).

9 Green, C. L. & Lamming, D. W. Regulation of metabolic health by essential dietary amino acids. *Mech Ageing Dev* **177**, 186-200, doi:10.1016/j.mad.2018.07.004 (2019).

10 Simpson, S. J. *et al.* Dietary protein, aging and nutritional geometry. *Ageing Res Rev* **39**, 78-86, doi:10.1016/j.arr.2017.03.001 (2017).

11 Grandison, R. C., Piper, M. D. & Partridge, L. Amino-acid imbalance explains extension of lifespan by dietary restriction in Drosophila. *Nature* **462**, 1061-1064, doi:10.1038/nature08619 (2009).

12 Miller, R. A. *et al.* Methionine-deficient diet extends mouse lifespan, slows immune and lens aging, alters glucose, T4, IGF-I and insulin levels, and increases hepatocyte MIF levels and stress resistance. *Aging Cell* **4**, 119-125, doi:10.1111/j.1474-9726.2005.00152.x (2005).

13 Yu, D. *et al.* Short-term methionine deprivation improves metabolic health via sexually dimorphic, mTORC1-independent mechanisms. *FASEB J* **32**, 3471-3482, doi:10.1096/fj.201701211R (2018).

14 Juricic, P., Gronke, S. & Partridge, L. Branched-chain amino acids have equivalent effects to other essential amino acids on lifespan and ageing-related traits in Drosophila. *J Gerontol A Biol Sci Med Sci*, doi:10.1093/gerona/glz080 (2019).

15 Fontana, L. *et al.* Decreased Consumption of Branched-Chain Amino Acids Improves Metabolic Health. *Cell Rep* **16**, 520-530, doi:10.1016/j.celrep.2016.05.092 (2016).

16 Solon-Biet, S. M. *et al.* Branched chain amino acids impact health and lifespan indirectly via amino acid balance and appetite control. *Nat Metab* **1**, 532-545, doi:10.1038/s42255-019-0059-2 (2019).

17 Lee, J., Seroogy, K. B. & Mattson, M. P. Dietary restriction enhances neurotrophin expression and neurogenesis in the hippocampus of adult mice. *J Neurochem* **80**, 539-547 (2002).

18 Cerletti, M., Jang, Y. C., Finley, L. W., Haigis, M. C. & Wagers, A. J. Short-term calorie restriction enhances skeletal muscle stem cell function. *Cell Stem Cell* **10**, 515-519, doi:10.1016/j.stem.2012.04.002 (2012).

19 Fan, P., Liu, P., Song, P., Chen, X. & Ma, X. Moderate dietary protein restriction alters the composition of gut microbiota and improves ileal barrier function in adult pig model. *Sci Rep* **7**, 43412, doi:10.1038/srep43412 (2017).

20 Regan, J. C. *et al.* Sex difference in pathology of the ageing gut mediates the greater response of female lifespan to dietary restriction. *Elife* **5**, e10956, doi:10.7554/eLife.10956 (2016).

21 Micchelli, C. A. & Perrimon, N. Evidence that stem cells reside in the adult Drosophila midgut epithelium. *Nature* **439**, 475-479, doi:10.1038/nature04371 (2006).

22 Ohlstein, B. & Spradling, A. The adult Drosophila posterior midgut is maintained by pluripotent stem cells. *Nature* **439**, 470-474, doi:10.1038/nature04333 (2006).

23 Biteau, B. *et al.* Lifespan extension by preserving proliferative homeostasis in Drosophila. *PLoS Genet* **6**, e1001159, doi:10.1371/journal.pgen.1001159 (2010).

24 Guo, L., Karpac, J., Tran, S. L. & Jasper, H. PGRP-SC2 promotes gut immune homeostasis to limit commensal dysbiosis and extend lifespan. *Cell* **156**, 109-122, doi:10.1016/j.cell.2013.12.018 (2014).

25 Fan, X. *et al.* Rapamycin preserves gut homeostasis during Drosophila aging. *Oncotarget* **6**, 35274-35283, doi:10.18632/oncotarget.5895 (2015).

26 Gronke, S., Clarke, D. F., Broughton, S., Andrews, T. D. & Partridge, L. Molecular evolution and functional characterization of Drosophila insulin-like peptides. *PLoS Genet* **6**, e1000857, doi:10.1371/journal.pgen.1000857 (2010).

27 Bjedov, I. *et al.* Mechanisms of life span extension by rapamycin in the fruit fly Drosophila melanogaster. *Cell Metab* **11**, 35-46, doi:10.1016/j.cmet.2009.11.010 (2010).

28 Zoncu, R., Efeyan, A. & Sabatini, D. M. mTOR: from growth signal integration to cancer, diabetes and ageing. *Nat Rev Mol Cell Biol* **12**, 21-35, doi:10.1038/nrm3025 (2011).

29 Shimobayashi, M. & Hall, M. N. Making new contacts: the mTOR network in metabolism and signalling crosstalk. *Nat Rev Mol Cell Biol* **15**, 155-162, doi:10.1038/nrm3757 (2014).

30 Chantranupong, L. *et al.* The Sestrins interact with GATOR2 to negatively regulate the amino-acid-sensing pathway upstream of mTORC1. *Cell Rep* **9**, 1-8, doi:10.1016/j.celrep.2014.09.014 (2014).

31 Lee, J. H., Budanov, A. V. & Karin, M. Sestrins orchestrate cellular metabolism to attenuate aging. *Cell Metab* **18**, 792-801, doi:10.1016/j.cmet.2013.08.018 (2013).

32 Budanov, A. V. & Karin, M. p53 target genes sestrin1 and sestrin2 connect genotoxic stress and mTOR signaling. *Cell* **134**, 451-460, doi:10.1016/j.cell.2008.06.028 (2008).

33 Wolfson, R. L. *et al.* Sestrin2 is a leucine sensor for the mTORC1 pathway. *Science* **351**, 43-48, doi:10.1126/science.aab2674 (2016).

34 Saxton, R. A. *et al.* Structural basis for leucine sensing by the Sestrin2-mTORC1 pathway. *Science* **351**, 53-58, doi:10.1126/science.aad2087 (2016).

35 Lee, J. H., Cho, U. S. & Karin, M. Sestrin regulation of TORC1: Is Sestrin a leucine sensor? *Sci Signal* **9**, re5, doi:10.1126/scisignal.aaf2885 (2016).

36 Lee, J. H. *et al.* Sestrin as a feedback inhibitor of TOR that prevents age-related pathologies. *Science* **327**, 1223-1228, doi:10.1126/science.1182228 (2010).

37 Arrese, E. L. & Soulages, J. L. Insect fat body: energy, metabolism, and regulation. *Annu Rev Entomol* **55**, 207-225, doi:10.1146/annurev-ento-112408-085356 (2010).

38 Scott, R. C., Schuldiner, O. & Neufeld, T. P. Role and regulation of starvation-induced autophagy in the Drosophila fat body. *Dev Cell* **7**, 167-178, doi:10.1016/j.devcel.2004.07.009 (2004).

39 Luis, N. M. *et al.* Intestinal IRE1 Is Required for Increased Triglyceride Metabolism and Longer Lifespan under Dietary Restriction. *Cell Rep* **17**, 1207-1216, doi:10.1016/j.celrep.2016.10.003 (2016).

40 Biteau, B., Hochmuth, C. E. & Jasper, H. JNK activity in somatic stem cells causes loss of tissue homeostasis in the aging Drosophila gut. *Cell Stem Cell* **3**, 442-455, doi:10.1016/j.stem.2008.07.024 (2008).

41 Rera, M., Clark, R. I. & Walker, D. W. Intestinal barrier dysfunction links metabolic and inflammatory markers of aging to death in Drosophila. *Proc Natl Acad Sci U S A* **109**, 21528-21533, doi:10.1073/pnas.1215849110 (2012).

42 Wang, X. & Proud, C. G. Nutrient control of TORC1, a cell-cycle regulator. *Trends Cell Biol* **19**, 260-267, doi:10.1016/j.tcb.2009.03.005 (2009).

43 Kamada, Y. *et al.* Tor directly controls the Atg1 kinase complex to regulate autophagy. *Mol Cell Biol* **30**, 1049-1058, doi:10.1128/MCB.01344-09 (2010).

44 Nagy, P., Varga, A., Kovacs, A. L., Takats, S. & Juhasz, G. How and why to study autophagy in Drosophila: it's more than just a garbage chute. *Methods* **75**, 151-161, doi:10.1016/j.ymeth.2014.11.016 (2015).

45 Nezis, I. P. *et al.* Autophagic degradation of dBruce controls DNA fragmentation in nurse cells during late Drosophila melanogaster oogenesis. *J Cell Biol* **190**, 523-531, doi:10.1083/jcb.201002035 (2010).

46 Williams, R. A., Smith, T. K., Cull, B., Mottram, J. C. & Coombs, G. H. ATG5 is essential for ATG8-dependent autophagy and mitochondrial homeostasis in Leishmania major. *PLoS Pathog* **8**, e1002695, doi:10.1371/journal.ppat.1002695 (2012).

47 Barnard, N. D. *et al.* A low-fat vegan diet and a conventional diabetes diet in the treatment of type 2 diabetes: a randomized, controlled, 74-wk clinical trial. *Am J Clin Nutr* **89**, 1588S-1596S, doi:10.3945/ajcn.2009.26736H (2009).

48 Lee, J. H. *et al.* Maintenance of metabolic homeostasis by Sestrin2 and Sestrin3. *Cell Metab* **16**, 311-321, doi:10.1016/j.cmet.2012.08.004 (2012).

49 Kim, M. *et al.* Sestrins are evolutionarily conserved mediators of exercise benefits. *Nat Commun* **11**, 190, doi:10.1038/s41467-019-13442-5 (2020).

50 Segales, J. *et al.* Sestrin prevents atrophy of disused and aging muscles by integrating anabolic and catabolic signals. *Nat Commun* **11**, 189, doi:10.1038/s41467-019-13832-9 (2020).

51 Kapahi, P. *et al.* Regulation of lifespan in Drosophila by modulation of genes in the TOR signaling pathway. *Curr Biol* **14**, 885-890, doi:10.1016/j.cub.2004.03.059 (2004).

52 Hahn, O. *et al.* Hepatic gene body hypermethylation is a shared epigenetic signature of murine longevity. *PLoS Genet* **14**, e1007766, doi:10.1371/journal.pgen.1007766 (2018).

53 Fok, W. C. *et al.* Combined treatment of rapamycin and dietary restriction has a larger effect on the transcriptome and metabolome of liver. *Aging Cell* **13**, 311-319, doi:10.1111/acel.12175 (2014).

54 Dobson, A. J. *et al.* Tissue-specific transcriptome profiling of Drosophila reveals roles for GATA transcription factors in longevity by dietary restriction. *Npj Aging Mech Dis* **4**, doi:UNSP 5
10.1038/s41514-018-0024-4 (2018).

55 Xi, J. *et al.* The TORC1 inhibitor Nprl2 protects age-related digestive function in Drosophila. *Aging (Albany NY)* **11**, 9811-9828, doi:10.18632/aging.102428 (2019).

56 Haller, S. *et al.* mTORC1 Activation during Repeated Regeneration Impairs Somatic Stem Cell Maintenance. *Cell Stem Cell* **21**, 806-818 e805, doi:10.1016/j.stem.2017.11.008 (2017).

57 Demetriades, C., Doumpas, N. & Teleman, A. A. Regulation of TORC1 in Response to Amino Acid Starvation via Lysosomal Recruitment of TSC2. *Cell* **156**, 786-799, doi:10.1016/j.cell.2014.01.024 (2014).

58 Amcheslavsky, A., Ito, N., Jiang, J. & Ip, Y. T. Tuberous sclerosis complex and Myc coordinate the growth and division of Drosophila intestinal stem cells. *Journal of Cell Biology* **193**, 695-710, doi:10.1083/jcb.201103018 (2011).

59 Kapuria, S., Karpac, J., Biteau, B., Hwangbo, D. & Jasper, H. Notch-Mediated Suppression of TSC2 Expression Regulates Cell Differentiation in the Drosophila Intestinal Stem Cell Lineage. *Plos Genetics* **8**, doi:ARTN e1003045

10.1371/journal.pgen.1003045 (2012).

60 Jasper, H. & Jones, D. L. Metabolic Regulation of Stem Cell Behavior and Implications for Aging. *Cell Metabolism* **12**, 561-565, doi:10.1016/j.cmet.2010.11.010 (2010).

61 Rodgers, J. T. *et al.* mTORC1 controls the adaptive transition of quiescent stem cells from G(0) to G(Alert). *Nature* **510**, 393-+, doi:10.1038/nature13255 (2014).

62 Ertl, R. P., Chen, J., Astle, C. M., Duffy, T. M. & Harrison, D. E. Effects of dietary restriction on hematopoietic stem-cell aging are genetically regulated. *Blood* **111**, 1709-1716, doi:10.1182/blood-2007-01-069807 (2008).

63 Rafalski, V. A. & Brunet, A. Energy metabolism in adult neural stem cell fate. *Prog Neurobiol* **93**, 182-203, doi:10.1016/j.pneurobio.2010.10.007 (2011).

64 Yousefi, M. *et al.* Calorie Restriction Governs Intestinal Epithelial Regeneration through Cell-Autonomous Regulation of mTORC1 in Reserve

Stem Cells. *Stem Cell Reports* **10**, 703-711, doi:10.1016/j.stemcr.2018.01.026 (2018).

65 Nagy, P., Sandor, G. O. & Juhasz, G. Autophagy maintains stem cells and intestinal homeostasis in Drosophila. *Sci Rep* **8**, 4644, doi:10.1038/s41598-018-23065-3 (2018).

66 Asano, J. *et al.* Intrinsic Autophagy Is Required for the Maintenance of Intestinal Stem Cells and for Irradiation-Induced Intestinal Regeneration. *Cell Reports* **20**, 1050-1060, doi:10.1016/j.celrep.2017.07.019 (2017).

67 Pan, H. Z., Cai, N., Li, M., Liu, G. H. & Belmonte, J. C. I. Autophagic control of cell "stemness'. *Embo Mol Med* **5**, 327-331, doi:10.1002/emmm.201201999 (2013).

68 Filer, D. *et al.* RNA polymerase III limits longevity downstream of TORC1. *Nature* **552**, 263-267, doi:10.1038/nature25007 (2017).

Figure Legends

Fig.1 Loss of *Sestrin* attenuates the response of lifespan to DR.

a,**b**, Survival (**a**) and median lifespan (**b**) of w^{Dah} and $Sesn^{3F6}$ females under DR. On 0.1x food and 2.0x SYA food, $Sesn^{3F6}$ flies showed similar lifespan to w^{Dah}, with P = 0.10 and P = 0.18, respectively, log rank test. On the 0.5x and 1.0x DR food, lifespan of $Sesn^{3F6}$ mutants was significantly reduced, with a decrease in median lifespan of 11% and 13%, respectively. P = 4.4E-5 (0.5x food), P = 4.8E-14 (1.0x food), log rank test. $Sesn^{3F6}$ flies responded to DR food significantly different from w^{Dah}, P < 0.0001, CPH analysis. N = 100 flies for each condition of each genotype. The lifespan assays were repeated twice.

Fig. 2 Generation of an amino acid sensing defective *Sestrin* fly mutant.

a, Partial sequence alignment of Sestrin proteins including the arginine (R) residue crucial for leucine binding (red). Sestrin2 from *H. sapiens* and *M. musculus* were used for the alignment. **b**, Structure of the *Drosophila* Sestrin protein modeled by UCSF Chimera on the human Sestrin2 protein (PDB: 5DJ4). The R407 residue (highlighted in red) is located in a pocket. **c**,**d**, Sestrin-GATOR2 *in vitro* interaction assays using the *Drosophila* wild type Sestrin protein and the *Drosophila* Sestrin R407A mutant protein (**c**). Branched chain amino acids and methionine interfered with Sestrin-GATOR2 interaction of the wild type Sestrin protein but not of the Sestrin R407A mutant protein. (**d**) Quantification of Sestrin protein associated with WDR24 protein in (**c**). Flag-WDR24 was used as loading control. Sestrin protein levels were normalized to the sample without amino acid addition. N = 3 independent experiments. **e**, CRISPR-Cas9 strategy to generate the Sestrin R407A mutation. A Myc tag (orange) was inserted

together with the R407A mutation (red). **f-i**, TORC1 activation upon amino acid induction in fat bodies of 3rd instar larvae. Fat bodies were starved for 1 hour and then stimulated with leucine (**f**,**g**) or all amino acids (**h**,**i**) for 10 min. Lysates were analyzed by immunoblotting. The Sestrin R407A mutation blocked TORC1 activation upon induction with leucine (**f**,**g**) and all amino acids (**h**,**i**). N = 4 biologically independent sets of samples. Two-way ANOVA analysis confirmed that *Sesn*^{R407A} mutants responded to addition of leucine and all amino acids significantly different from wild type fat bodies ($P < 0.05$). Data in (**d**, **g**, **i**) are presented as mean +/- SEM. Statistics in (**d**, **g**, **i**): Two-way ANOVA with Bonferroni's post-hoc test, P values were adjusted for multiple comparisons.

Fig. 3 The *Sesn*^{R407A} mutation impairs growth, increases lifespan, and blunts high protein diet induced lifespan shortening.

a-c, *Sesn*^{R407A} mutant flies showed reduced TORC1 activity. Fat body tissues from 3rd instar larvae grown under standard conditions were subjected to immunoblotting analysis. pS6K was normalized to total S6K, and pAKT to total AKT. pS6K, but not pAKT was downregulated in *Sesn*^{R407A} mutant fat body tissues. N = 3 biologically independent samples. Data in (**b**, **c**) are presented as mean +/- SEM. Unpaired, two-tailed t-test. **d**, *Sesn*^{R407A} mutant flies were developmentally delayed. Percentage eclosion at indicated time points. N = 10 vials with 50 embryos per vial. Data are presented as mean +/- SEM. Permutation test showed that *Sesn*^{R407A} mutants emerged significantly later than wild type flies. P value was adjusted for multiple testing. **e**, Wet weight of newly emerged flies. N = 20 pairs of flies. Median, 25th and 75th percentiles, and Tukey whiskers are indicated. Unpaired, two-tailed t-test. **f**,**g**, Survival (**f**) and median lifespan (**g**) of *Sesn*^{wt} and *Sesn*^{R407A} females under DR. Lifespan of *Sesn*^{R407A}

mutant flies was slightly extended under DR conditions with a median lifespan increase of 11%, 14% on the 0.5x and 1.0x DR food, respectively. On the 2.0x food under fully fed conditions, however, $Sesn^{R407A}$ mutant females showed a strong increase in lifespan with an increase in median lifespan of 40%. P = 0.34 (0.1x food), P = 9.8E-5 (0.5x food), P = 9.0E-8 (1.0x food), P = 1.8E-20 (2.0x food), log rank test. $Sesn^{R407A}$ flies responded to DR food significantly differently from control flies, P < 0.0001, CPH analysis. N = 100 flies for each condition of each genotype. The DR lifespan assay was performed once, and 1.0x condition was independently repeated.

Fig. 4 Sestrin is important for maintenance of intestinal stem cells in response to DR.

a,**b**, Gut stem cell activity of w^{Dah} and $Sesn^{3F6}$ flies under DR. (**a**) Representative images from 20-day old flies. Actively dividing stem cells are indicated by arrows. (**b**) Quantification of pH3-positive cells in $Sesn^{3F6}$ females under DR. N = 25 guts (w^{Dah}, $Sesn^{3F6}$, 2.0x; $Sesn^{3F6}$, 1.0x), N = 24 guts (w^{Dah}, 1.0x). **c**,**d**, Gut turnover rates upon *Sestrin* knockdown. (**c**) Representative images after 7-day induction. (**d**) Quantification of gut turnover rates in *Sestrin* knockdown flies under DR. N = 14 guts (w^{Dah}, 2.0x, 1.0x), N = 16 guts (*Sesn KD*, 2.0x), N = 17 guts (*Sesn KD*, 1.0x). **e**,**f**, Gut stem cell activity of $Sesn^{R407A}$ mutant flies under DR conditions. (**e**) Representative images from 20-day old flies. (**f**) Quantification of pH3-positive cells in $Sesn^{R407A}$ mutants under DR. N = 25 guts ($Sesn^{wt}$, 2.0x, 1.0x), N = 24 guts ($Sesn^{R407A}$, 2.0x, 1.0x). **g**,**h**, Gut turnover rates in $Sesn^{R407A}$ mutant flies under DR. (**g**) Representative images after 7-day induction. (**h**) Quantification of gut turnover rates in $Sesn^{R407A}$ mutants under DR. N = 14 guts ($Sesn^{wt}$, 2.0x; $Sesn^{R407A}$, 1.0x), N = 15 guts ($Sesn^{wt}$, 1.0x; $Sesn^{R407A}$, 2.0x). **i**,**j**, Quantification of gut turnover rates in $Sesn^{R407A}$ mutants upon addition of all amino

acids (**i**) and addition of methionine and branched chain amino acids (MBC) (**j**). N = 13 guts (**i**), N = 16 guts (**j**). Scale bar represents 50 μm. Median, 25th and 75th percentiles, and Tukey whiskers are indicated in box-and-whisker plots (**b**, **d**, **f**, **h**-**j**). Outliers are shown as open circles. Interaction between diet and genotype was significant in (**b**, **d**, **f**, **h**-**j**): two-way ANOVA, P = 0.02 (**b**), P = 0.01 (**d**), P = 0.02 (**f**), P = 0.01 (**h**), P < 0.0001 (**i**), P = 0.047 (**j**). Statistics in (**b**, **d**, **f**, **h**-**j**): Two-way ANOVA followed by Bonferroni's post-hoc test, P values were adjusted for multiple comparisons.

Fig. 5 *Sestrin* over-expression in gut stem cells improves gut homeostasis.

a,**b**, Ubiquitous over-expression of *Sestrin* reduced gut stem cell activity. (**a**) Representative images from 30-day old flies without (RU486-) or with (RU486+) induction. Actively dividing stem cells are indicated by arrows. Scale bar: 50 μm. (**b**) Quantification of pH3-positive cells on days 10, 30 and 50. N = 20 guts (RU486-), N = 22 guts (RU486+), day 10; N = 23 guts (RU486-, RU486+), day 30; N = 24 guts (RU486-, RU486+), day 50. GLM analysis confirmed that *Sestrin* over-expression significantly reduced the increase in age dependent stem cell activity (P = 0.012). **c**,**d**, Over-expression of *Sestrin* in enterocytes (*5966GS*) did not affect pH3-positive cell numbers (**c**). Day 30: N = 22 guts (RU486-), N = 21 guts (RU486+); day 46: N = 22 guts (RU486-), N = 20 guts (RU486+). In contrast, over-expression of *Sestrin* in gut stem cells (*5961GS*) significantly reduced stem cell activity (**d**). Day 30: N = 24 guts (RU486-), N = 25 guts (RU486+); day 46: N = 22 guts (RU486-), N = 23 guts (RU486+). **e**, *Sestrin* over-expression prolonged the G1 phase in gut stem cells. Fly-Fucci and *Sestrin* were driven by the *esg-Gal4* driver. *Sestrin* over-expression significantly changed cell cycle distribution of gut stem cells. N = 416 cells, w^{Dah}; N = 382 cells,

Sesn OE. Chi-square test. **f-h**, *Sestrin* over-expression in gut stem cells decreased gut dysplasia (**f**,**g**) and the proportion of Smurf flies (**h**). (**f**) Representative gut images from 50-day old flies. DNA (DAPI) in blue. The gut epithelium is indicated by dashed lines. Scale bar represents 20 μm. (**g**) The difference in gut dysplasia was significant. N = 13 guts. (**h)** Flies were 60-day old. N = 15 guts. Median, 25th and 75th percentiles, and Tukey whiskers are indicated in box-and-whisker plots (**b**-**d**, **g**, **h**). Outliers are shown as open circles. Statistics in (**b**, **c**, **d**): two tailed, Mann Whitney test; statistics in (**g, h**): Unpaired, two-tailed t-test.

Fig. 6 Sestrin regulates lifespan and stem cell maintenance via the TOR pathway. **a**,**b**, Survival of *Sestrin* mutant females under rapamycin treatment. (**a**) Untreated $Sesn^{3F6}$ flies were short-lived (P = 3.7E-8, log rank test). Rapamycin treatment increased median lifespan of w^{Dah} and $Sesn^{3F6}$ females by 13% and 21%, respectively. P = 6.4E-11 (w^{Dah}), P = 2.1E-29 ($Sesn^{3F6}$), log rank test. Lifespan of w^{Dah} and $Sesn^{3F6}$ flies under rapamycin treatment was not significantly different (P = 0.30, log rank test). $Sesn^{3F6}$ flies responded to rapamycin treatment significantly different from w^{Dah}, P < 0.001, CPH analysis. (**b**) Lifespan of $Sesn^{wt}$ but not of $Sesn^{R407A}$ mutants, was significantly increased by rapamycin treatment. P = 1.0E-06 ($Sesn^{wt}$), P = 0.37 ($Sesn^{R407A}$), log rank test. Lifespan of $Sesn^{wt}$ and $Sesn^{R407A}$ flies under rapamycin treatment was not significantly different (P = 0.13, log rank test). $Sesn^{R407A}$ flies responded to rapamycin treatment significantly different from $Sesn^{wt}$, P < 0.001, CPH analysis. N = 150 flies. Experiments were performed once. **c**-**f**, Gut stem cell activity of controls and *Sesn* mutant flies under rapamycin treatment. (**c**,**e**) Representative gut images from 30-day old flies. Actively dividing stem cells are indicated by arrows. (**d**,**f**) Quantification of pH3-positive cells in $Sesn^{3F6}$ mutant flies (**d**) and in $Sesn^{R407A}$ mutant

flies (**f**) under rapamycin treatment. N = 21 guts (**d**), N = 20 guts (**f**). Interaction between genotype and drug treatment was significant: two-way ANOVA, P = 0.0175 (**d**), P = 0.001 (**f**). **g-j**, Gut cell turnover rates under rapamycin treatment upon knockdown or over-expression of *Sestrin*. (**g**,**i**) Representative images after 10-day induction. (**h**,**j**) Quantification of gut cell turnover rates in *Sestrin* knockdown (**h**) and over-expression (**j**) flies under rapamycin treatment. N = 18 guts (**h**, **j**). The interaction between drug treatment and genotype was significant (Two-way ANOVA, P < 0.0001) (**h**, **j**). Scale bar represents 50 μm. Median, 25th and 75th percentiles, and Tukey whiskers are indicated in box-and-whisker plots (**d**, **f**, **h**, **j**). Outliers are shown as open circles. Statistics in (**d**, **f**, **h**, **j**): Two-way ANOVA followed by Bonferroni's post-hoc test, P values were adjusted for multiple comparisons.

Fig. 7 Sestrin increases autophagy in ISCs to regulate gut cell turnover.

a,**b**, *Sestrin* over-expression induced autophagy in gut stem cells. Stem cells were marked by GFP (green), DNA by DAPI (blue), and autophagy by mCherry::Atg8a (gray). Representative images from 10-day old females. Scale bars: 5 μm. N = 5 guts. Data are presented as mean +/- SEM. Unpaired, two-tailed t-test. **c**,**d**, Autophagy is an essential downstream mediator of Sestrin function in ISCs. (**c**) Representative images after 10 days of induction. Scale bar represents 50 μm. (**d**) *Atg1* over-expression in ISCs reduced gut turnover rates and there was no additive effect when combined with *Sestrin* over-expression. *Sestrin* over-expression significantly reduced gut cell turnover rate, and this effect was blocked by *Atg5* knockdown. N = 16 guts (w^{Dah}, *Sesn OE*, *Atg1 OE*, *Sesn OE* + *Atg1 OE*), N= 18 guts (*Atg5 KD*, *Sesn OE* + *Atg5 KD*). Gut cell turnover rates of *Sestrin* over-expression flies showed a significantly different response to *Atg1* over-expression (Two-way ANOVA, P = 0.0001) and *Atg5* knockdown (Two-way

ANOVA, P = 0.0023) than that of wild type flies. Median, 25th and 75th percentiles, and Tukey whiskers are indicated in box-and-whisker plots (**d**). Outliers are shown as open circles. Statistics in (**d**): Two-way ANOVA followed by Bonferroni's post-hoc test, P values were adjusted for multiple comparisons.

Fig. 8 *Sestrin* over-expression in gut stem cells extends lifespan.

a, Median lifespan of female flies with adult-onset ubiquitous over-expression of *Sestrin* using the *daGS* driver was increased by 10% compared to the non-induced control (P = 2.2E-5, log rank test). **b-d**, Adult-onset over-expression of *Sestrin* in the adult nervous system (*elavGS*) (**b**) (P = 0.82, log rank test), the adult fat body (*S$_1$106GS*) (**c**) (P = 0.15, log rank test) or gut enterocytes (*5966GS*) (**d**) (P = 0.09, log rank test) did not affect lifespan. **e**, Over-expression of *Sestrin* in gut stem cells (*5961GS*) significantly increased lifespan, with a median lifespan increase of 10% (P = 4.2E-4, log rank test). Lifespans in (**a**-**e**) were performed on 1.0x SYA. **f**, Over-expression of *Sestrin* in gut stem cells increased median lifespan by 15% on a high yeast diet (2.0x SYA) (P = 5.4E-6, log rank test). N = 100 flies (**a**-**e**), N = 120 flies (**f**). Experiment (**a**) was repeated three times, (**e**) twice, and others once.

Methods

Fly stocks and husbandry

All fly stocks were backcrossed for at least six generations into the w^{Dah} background, with the exception of tool chromosomes in the clonal assay[69], the gut turnover assay[70] and the Fly-Fucci system[71]. Flies were maintained on 1.0x SYA (10% (w/v) brewer's yeast, 5% (w/v) sucrose, and 1.5% (w/v) agar) food at 25°C, 60% humidity, on a 12-hour light and 12-hour dark cycle condition, unless otherwise noted. To induce gene expression using the Gene-Switch system[72], RU486 (Sigma, Cat# M8046) was added to the food at a final concentration of 200 μM. Rapamycin (LC Laboratories, Cat# R-5000) was added to the food at a final concentration of 200 μM. Female flies were used unless otherwise noted. The fly stocks used in this study are listed in Supplementary Table 1, and the genotypes of flies in each figure are listed in Supplementary Table 2.

Sequence alignment and structure modeling

Sestrin protein sequence alignment was performed using the PROMALS3D method[73]. Sequences of each species used in the analysis were as follows: UniProt: Q5W1K5 (*D. melanogaster*), UniProt: P58004 (*H. Sapiens*), UniProt: P58043 (*M. musculus*), UniProt: Q6NU55 (*X. laevis*), UniProt: A0F081 (*D. rerio*), UniProt: Q9N4D6 (*C. elegans*). Sestrin protein structure was modeled using UCSF Chimera V1.12.0[74]. Human Sestrin2 protein structure (PDB: 5DJ4) was used as modeling template.

Generation of mutant and transgenic fly lines

To generate the transgenic *UAS-Sestrin* fly line, the full-length *Sestrin* cDNAs were amplified by PCR from BDGP DGC clone (LD39604) and cloned into *pUAST-attB*

vector[75]. φC31-mediated transgenesis[75] was used to generate transgenic flies, using the *attP2* insertion site[76]. The *Sesn*^{wt} and *Sesn*^{R407A} fly lines were generated by a fully transgenic CRISPR/Cas9 approach using two guide RNAs (gRNAs)[77] targeting the *Sestrin* gene locus. The gRNAs were amplified by PCR using the *pCDF4* plasmid as template, followed by its cloning into the *pCDF4* vector using the Gibson Assembly kit (NEB, Cat# E2611S). The resulting plasmid was then introduced to *attP40* insertion site[76] to generate *Sestrin*-gRNA transgenic flies. The *Sestrin* donor constructs contained the following elements: left homologous arm (1045 bp); PAM site (mutated to NheI); R407 region (3718 bp); tag region (679 bp); PAM site (mutated to KpnI); right homologous arm (1015 bp). These fragments were amplified from BAC clone (BACR02E09) and cloned into *pOT2* vector[78]. The *Myc* tag was introduced using sequences in primers, and the *Sestrin* R407A mutation was generated by site-directed mutagenesis (Agilent). To generate *Sesn*^{wt} and *Sesn*^{R407A} mutant flies, flies expressing the two gRNAs were crossed with flies expressing *Cas9* under the ubiquitous actin promotor, and their progeny embryos were injected with the *Sesn*^{wt}*::myc* and *Sesn*^{R407A}*::myc* donor constructs. PCR screening targeting the *Myc* tag sequence was used to identify positive lines and the presence of the R407A mutation was confirmed by sequencing. Primers used for cloning are listed in Supplementary Table 3.

Development time and adult weight

For development time analysis, flies were allowed to lay eggs for 60 mins, and these were transferred to vials at a density of 40 or 50 per vial, as indicated in each experiment. The number of flies eclosed was then recorded. For body weight measurements of adult flies, 40 flies that eclosed within 12-hour were anesthetized and weighted in pairs on an ME235S genius balance (Sartorius).

Lifespan, dietary restriction, and fecundity

For lifespan assays, flies were reared at standard larval density (20µl embryos = ~300 eclosed flies, per bottle). Eclosed flies were allowed to mate for 2 days, and then sorted into vials. Flies were transferred to fresh vials every two to three days and scored for deaths. 1.0x SYA food was used in most experiments. For DR experiments, the yeast content of the diet was diluted with 2.0x SYA containing 200g yeast/l food, 1.0x SYA 100g yeast/l food, 0.5x SYA 50g yeast/l food, 0.1x SYA 10g yeast/l food[26]. Details of all lifespan trials are listed in Supplementary Table 4 and 5. For the fecundity assay, eggs laid in a period of 3-6 hours within the first 4 weeks of adulthood were collected and counted, twice a week in the first two weeks and once a week in the next two weeks.

qRT-PCR

Total RNA was extracted from flies using Trizol (Invitrogen, Cat# 15596018) following the manual. RNA concentration was measured by Nanodrop One (Thermo Scientific). cDNA synthesis was performed using the SuperScript III first-strand synthesis kit (Invitrogen, Cat# 18080-400) with random hexamers and 600 ng of total RNA as input. SYBR Green Master Mix (Applied Biosystems, Cat# 4367659) was used and samples were prepared with the Janus automated workstation (PerkinElmer). qPCR was performed using the QuantStudio 6 Flex real-time PCR system with Real-Time PCR Software V1.1 (Life Technologies). Relative expression levels were determined using the ΔΔCT method, and *Rpl32* was used for normalization. Primers for qRT-PCR are listed in Supplementary Table 3.

Sestrin-GATOR2 interaction assay

HEK-293T cells (ATCC, Cat# CRL-3216) were cultured in Dulbecco's Modified Eagle Medium (DMEM, Gibco, Cat# 41965039) supplemented with 10% Fetal Bovine Serum (FBS, Gibco, Cat# 10270-106), 50 units/ml penicillin and 50 μg/ml streptomycin (Gibco, Cat# 15070-063). Cells were maintained at 37°C in a 5% CO_2 incubator (Thermo Scientific). HEK-293T cells were plated in 10 cm plates one day before transfection. Cell transfection was performed using polyethylenimine (Sigma, Cat# 408727) with *pcDNA3*-based plasmids expressing fly cDNAs (*WDR24* cDNA source: BDGP DGC clone LD21720) for *Flag-WDR24* and *HA-Sestrin*^{wt} or *HA-Sestrin*^{R407A}. The transfected mounts for each plate were as follows: 5 μg of DNA per vector (total 10 μg) was used for transfection. 48 hours after transfection, cells were starved for all amino acids for 50 mins and then harvested. Cells were lysed with Triton lysis buffer containing 1% Triton X-100, 50 mM Tris-HCl (pH8.0), 150 mM NaCl, 2.5 mM $MgCl_2$, and 1x Complete protease inhibitors (Roche, Cat# 11836170001) and 1x PhosSTOP phosphatase inhibitors (Roche, Cat# 04906837001). Cell lysates from the same type of transfected cell plates were combined, mixed and then equally distributed to test tubes. Individual amino acids were added to the cell lysate at a final concentration of 2 mM, a concentration within the physiological range for most essential amino acids in *Drosophila* cells (Supplementary Table 6). Anti-Flag microbeads were added to cell lysate, followed by incubation with rotation for 2 hours at RT. Anti-Flag immunoprecipitation was performed according to the manual of the μMACS Flag Isolation Kit (Miltenyi Biotec, Cat# 130-101-591) with the wash buffer containing 1% Triton X-100, 50 mM Tris-HCl (pH8.0), 500 mM NaCl, 2.5 mM $MgCl_2$. Immunoprecipitated proteins were analyzed by immunoblotting using antibodies against Flag and HA tag.

Amino acid concentration measurement in cultured cells

Drosophila S2R+ cells (DGRC, Cat# 150, CVCL_Z831) were cultured in Schneider's Drosophila Medium (Thermo Fisher Scientific, Cat# 21720024) supplemented with 10% Fetal Bovine Serum (FBS, Gibco, Cat# 10270-106), 50 units/ml penicillin and 50 μg/ml streptomycin (Gibco, Cat# 15070-063). Cells were maintained at 25°C in an incubator (Thermo Scientific). Cells were incubated in fresh medium for 2 hours and harvested. Number and diameter of cells were measured by Vi-CELL XR cell viability analyzer with software 2.04 (Beckman Coulter). The harvested cell pellets were subjected to LC-MS analysis. Identity of each compound was validated by authentic reference compounds. Data analysis of the measured amino acids was performed using the TraceFinder software (V4.2, Thermo Fisher Scientific). Amino acid concentration was calculated based on the amount of amino acids and the cell numbers and volumes of samples.

Amino acid starvation and stimulation

Amino-acid-free or -containing media were made based on the formula of Schneider's *Drosophila* medium (1x, Thermo Fisher Scientific, Cat# 21720024). Stock solutions were made and mixed to get a final 1x medium. Fat bodies were dissected in Schneider's *Drosophila* medium within 30 min. Samples were rinsed twice with amino-acid-free medium and then incubated for 1 hour in the same medium. Amino acid stimulation was performed by addition of medium containing only leucine (final concentration, 3g/l, 20x) or by addition of medium containing all amino acids (final concentration, 1x) for 10 min. Samples were immediately lysed in Laemmli buffer and subjected to immunoblotting analysis.

Immunoblotting

Tissues were lysed in the RIPA buffer or the Laemmli buffer with addition of 2x Complete protease inhibitors (Roche, Cat# 11836170001) and 2x PhosSTOP phosphatase inhibitors (Roche, Cat# 04906837001). Protein extracts were resolved using SDS-PAGE and transferred to Immobilon-FL PVDF membranes (Merck, Cat# IPFL00010). Blots were blocked in Odyssey blocking buffer (LI-COR, Cat# 927-50000) for 1 hour and probed with the following antibodies: anti-Sestrin (1:1000), anti-Myc (1:1000), anti-Flag (1:1000), anti-HA (1:1000), anti-pS6K T398 (1:1000), anti-S6K (1:1000), anti-Tubulin (1:5000), anti-pAMPKα T172 (1:1000), anti-pAKT S505 (1:1000), anti-AKT (1:1000), goat anti-rabbit IgG IRDye 680RD (1:15000), goat anti-mouse IgG IRDye 800CW (1:15000). Detection and quantification were performed using the Odyssey Infrared Imaging system with application software V3.0.30 (LI-COR). The sources of antibodies used are listed in Supplementary Table 7.

Immunofluorescence

Tissues were dissected in PBS and collected on ice. Samples were fixed 30 min with 4% formaldehyde (Thermo Scientific, Cat# 28908) and blocked with 5% non-fat milk for at least 2 hours at room temperature. Primary antibody incubation was at 4°C overnight, followed by secondary antibody incubation for at least 2 hours at room temperature. The antibodies used were the following: anti-pH3 (1:200), goat anti-rabbit IgG, AF594 (1:1000). The sources of antibodies used are listed in Supplementary Table 7. Samples were mounted in Vectashield mounting medium containing DAPI (Vector Laboratories, Cat# H-1200). Imaging was performed using Leica TCS SP5-X, SP8-X confocal microscopes.

FLP/FRT clonal assay and gut turnover assay

For fat body *FLP/FRT* clonal assay[69], eggs laid overnight were heat-shocked at 37°C for 1 hour. Fat bodies from wandering 3rd instar larvae were dissected and fixed in 4% formaldehyde (Thermo Scientific, Cat# 28908). Samples were stained with Phalloidin CF594 (1:40, Biotium, Cat# 00045) for 30 mins and mounted. For gut turnover assay, the *esg^{ts} F/O* flies (w; *esg-Gal4, tubGal80^{ts}, UAS-GFP; UAS-flp, Act>CD2>Gal4*) were used[70]. Crosses were set up and progeny were raised at 18°C. 4-day old females were sorted and shifted to 29°C for indicated days. For amino acid adding back to 1.0x SYA diet, the amount of amino acids was based on previous study[11]. Guts were dissected, fixed in 4% formaldehyde (Thermo Scientific, Cat# 28908), and mounted. Samples were imaged using Leica TCS SP5-X, SP8-X confocal microscopes with focus on R4-R5 region of the gut, and images were analyzed using ImageJ 1.51m9.

Gut dysplasia and Smurf assay

Flies were maintained at indicated conditions and aged until the day of assays. For gut dysplasia assay, guts were dissected, fixed for 30 min with 4% formaldehyde (Thermo Scientific, Cat# 28908), and then mounted to slides with Vectashield mounting medium containing DAPI (Vector Laboratories, Cat# H-1200). Samples were imaged using Leica TCS SP8-X confocal microscopes with focus on the R2 region of the gut. Images were analyzed using ImageJ. Proportion of dysplasia was scored as the ratio between length of gut epithelium with several layers of nuclei and total length of the gut. For Smurf assay, flies were transferred to standard SYA food containing 1.2% (w/v) blue dye (Sigma, Cat# 861146) for 48 hours. If the dye leaked outside of the gut, it was scored as Smurf.

Statistics and reproducibility

No statistical methods were used to pre-determine sample sizes but our sample sizes are similar to those reported in previous publications[20,23,68]. Samples were allocated to groups/treatments randomly, and steps were taken to avoid batch effects. Experimental conditions were not blinded. However, data analysis was performed blind whenever possible. No data were excluded from the analysis. The times of experiments independently repeated were indicated in relevant figure legends for lifespan assays, and for other assays experiments were performed once with indicated setups. Data were analyzed using the GraphPad Prism 6, JMP 10, R 3.3.1 or Excel 2013 software. For development time assays, data were analyzed using permutation test (R, statmod package). For lifespan assays, data were recorded in Excel, and a log rank test was performed. Cox-proportional hazard (CPH) analysis was performed using JMP software (SAS). Data presented Fig. 5b-d and in Extended Data Fig. 3e,f were not normally distributed, thus a Mann Whitney test was used for the analysis. Other data distribution was assumed to be normal but this was not formally tested. For small sample sizes ($N < 10$), data were presented with mean +/- SEM with individual data point shown. For samples with large sizes ($N \geq 10$), box-and-whisker plots were used with median, 25th and 75th percentiles, and Tukey whiskers indicated in plots. Outliers are shown as open circles. P values less than 0.05 are considered to be statistically significant, and exact P values are provided whenever possible in figures or figure legends. Additional details, including F values, t values, and degrees of freedom for relevant tests can be found in the statistical Source Data files.

Reporting Summary

Further information on the experimental design is available in the Nature Research Reporting Summary linked to this article.

Data availability

Statistical source data corresponding to each figure are provided as Excel tables. Unprocessed immunoblots are provided as source data. The structure of human Sestrin2 (Uniprot: P58004) used to model the structure of the fly Sestrin protein (Uniprot: Q9W1K5) is PDB: 5DJ4 (DOI: 10.2210/pdb5DJ4/pdb). All data that support the findings of this study are available from the corresponding authors upon request.

Reference

69 Theodosiou, N. A. & Xu, T. Use of FLP/FRT system to study Drosophila development. *Methods* **14**, 355-365, doi:10.1006/meth.1998.0591 (1998).

70 Jiang, H., Grenley, M. O., Bravo, M. J., Blumhagen, R. Z. & Edgar, B. A. EGFR/Ras/MAPK signaling mediates adult midgut epithelial homeostasis and regeneration in Drosophila. *Cell Stem Cell* **8**, 84-95, doi:10.1016/j.stem.2010.11.026 (2011).

71 Zielke, N. *et al.* Fly-FUCCI: A versatile tool for studying cell proliferation in complex tissues. *Cell Rep* **7**, 588-598, doi:10.1016/j.celrep.2014.03.020 (2014).

72 Roman, G., Endo, K., Zong, L. & Davis, R. L. P[Switch], a system for spatial and temporal control of gene expression in Drosophila melanogaster. *Proc Natl Acad Sci U S A* **98**, 12602-12607, doi:10.1073/pnas.221303998 (2001).

73 Pei, J., Kim, B. H. & Grishin, N. V. PROMALS3D: a tool for multiple protein sequence and structure alignments. *Nucleic Acids Res* **36**, 2295-2300, doi:10.1093/nar/gkn072 (2008).

74 Pettersen, E. F. *et al.* UCSF Chimera--a visualization system for exploratory research and analysis. *J Comput Chem* **25**, 1605-1612, doi:10.1002/jcc.20084 (2004).

75 Bischof, J., Maeda, R. K., Hediger, M., Karch, F. & Basler, K. An optimized transgenesis system for Drosophila using germ-line-specific phiC31 integrases. *Proc Natl Acad Sci U S A* **104**, 3312-3317, doi:10.1073/pnas.0611511104 (2007).

76 Markstein, M., Pitsouli, C., Villalta, C., Celniker, S. E. & Perrimon, N. Exploiting position effects and the gypsy retrovirus insulator to engineer precisely expressed transgenes. *Nat Genet* **40**, 476-483, doi:10.1038/ng.101 (2008).

77 Port, F., Chen, H. M., Lee, T. & Bullock, S. L. Optimized CRISPR/Cas tools for efficient germline and somatic genome engineering in Drosophila. *Proc Natl Acad Sci U S A* **111**, E2967-2976, doi:10.1073/pnas.1405500111 (2014).

78 Rubin, G. M. *et al.* A Drosophila complementary DNA resource. *Science* **287**, 2222-2224, doi:10.1126/science.287.5461.2222 (2000).

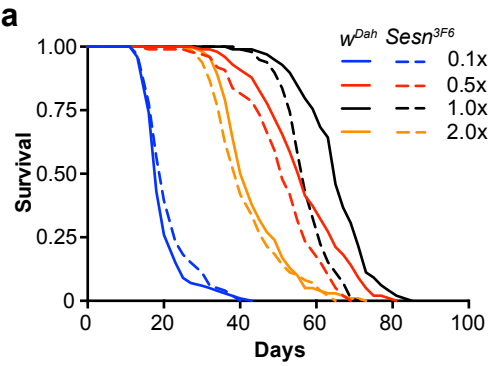
a
w^Dah Sesn^3F6
0.1x
0.5x
1.0x
2.0x
Survival
1.00
0.75
0.50
0.25
0
0
20
40
60
80
100
Days

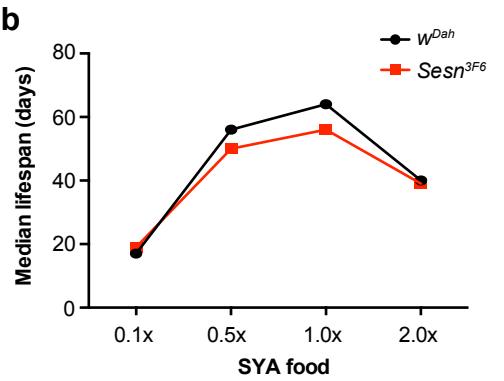
b
w^Dah
Sesn^3F6
Median lifespan (days)
80
60
40
20
0
0.1x
0.5x
1.0x
2.0x
SYA food

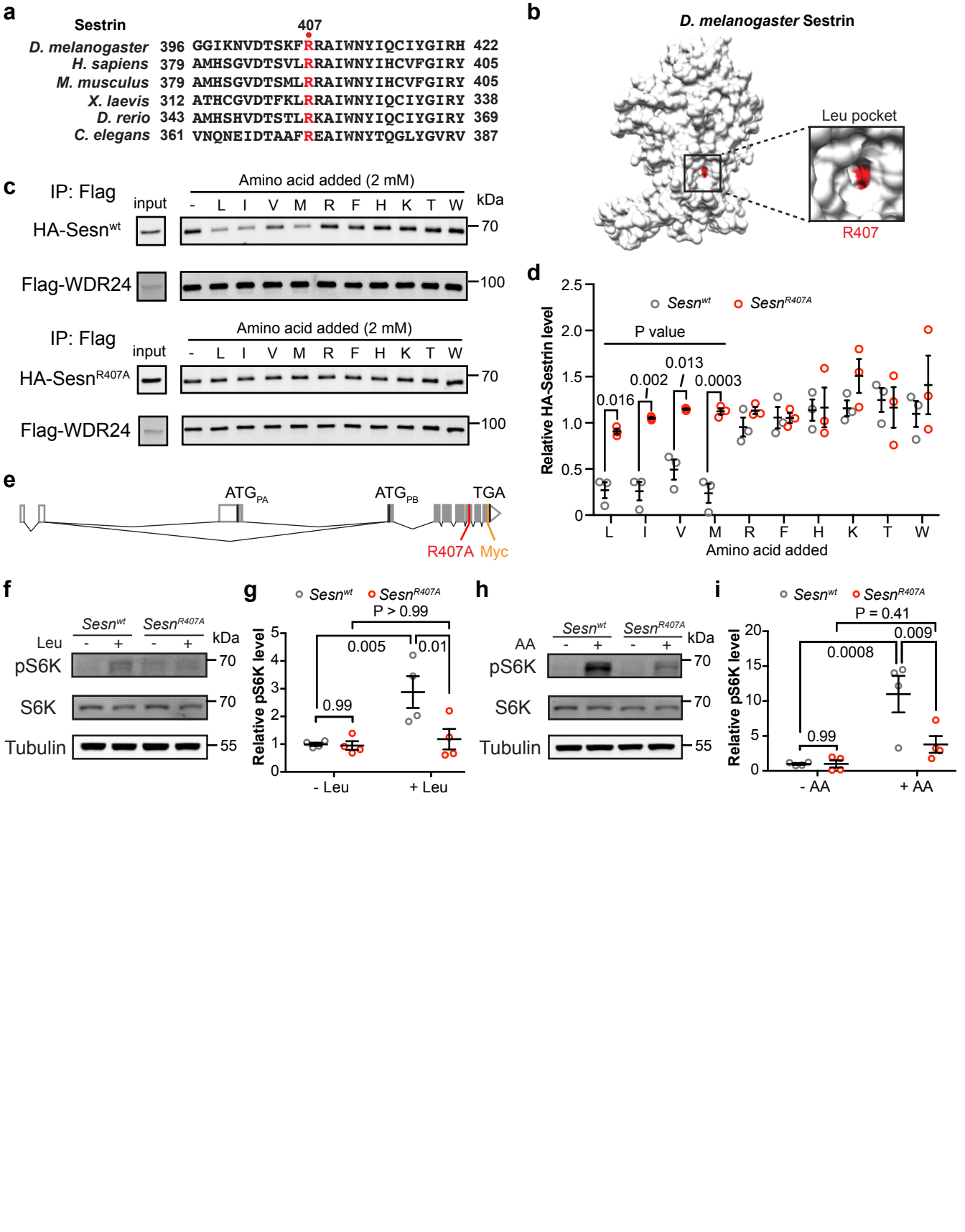
a
Sestrin
407
D. melanogaster 396 GGIKNVDTSKFRRAIWNYIQCIYGIRH 422
H. sapiens 379 AMHSGVDTSVLRRAIWNYIHCVFGIRY 405
M. musculus 379 AMHSGVDTSMLRRAIWNYIHCVFGIRY 405
X. laevis 312 ATHCGVDTFKLRRAIWNYIQCIYGIRY 338
D. rerio 343 AMHSHVDTSTLRKAIWNYIQCIYGIRY 369
C. elegans 361 VNQNEIDTAAFREAIWNYTQGLYGVRV 387
b
D. melanogaster Sestrin
Leu pocket
R407
c
IP: Flag
input
Amino acid added (2 mM)
- L I V M R F H K T W
kDa
HA-Sesn^wt
70
Flag-WDR24
100
IP: Flag
input
Amino acid added (2 mM)
- L I V M R F H K T W
HA-Sesn^R407A
70
Flag-WDR24
100
d
Sesn^wt
Sesn^R407A
P value
0.016
0.002
0.013
0.0003
Relative HA-Sestrin level
Amino acid added
L I V M R F H K T W
e
ATG_PA
ATG_PB
TGA
R407A
Myc
f
Sesn^wt
Sesn^R407A
Leu
- + - +
kDa
pS6K
70
S6K
70
Tubulin
55
g
Sesn^wt
Sesn^R407A
P > 0.99
0.005
0.01
0.99
Relative pS6K level
- Leu
+ Leu
h
Sesn^wt
Sesn^R407A
AA
- + - +
kDa
pS6K
70
S6K
70
Tubulin
55
i
Sesn^wt
Sesn^R407A
P = 0.41
0.009
0.0008
0.99
Relative pS6K level
- AA
+ AA

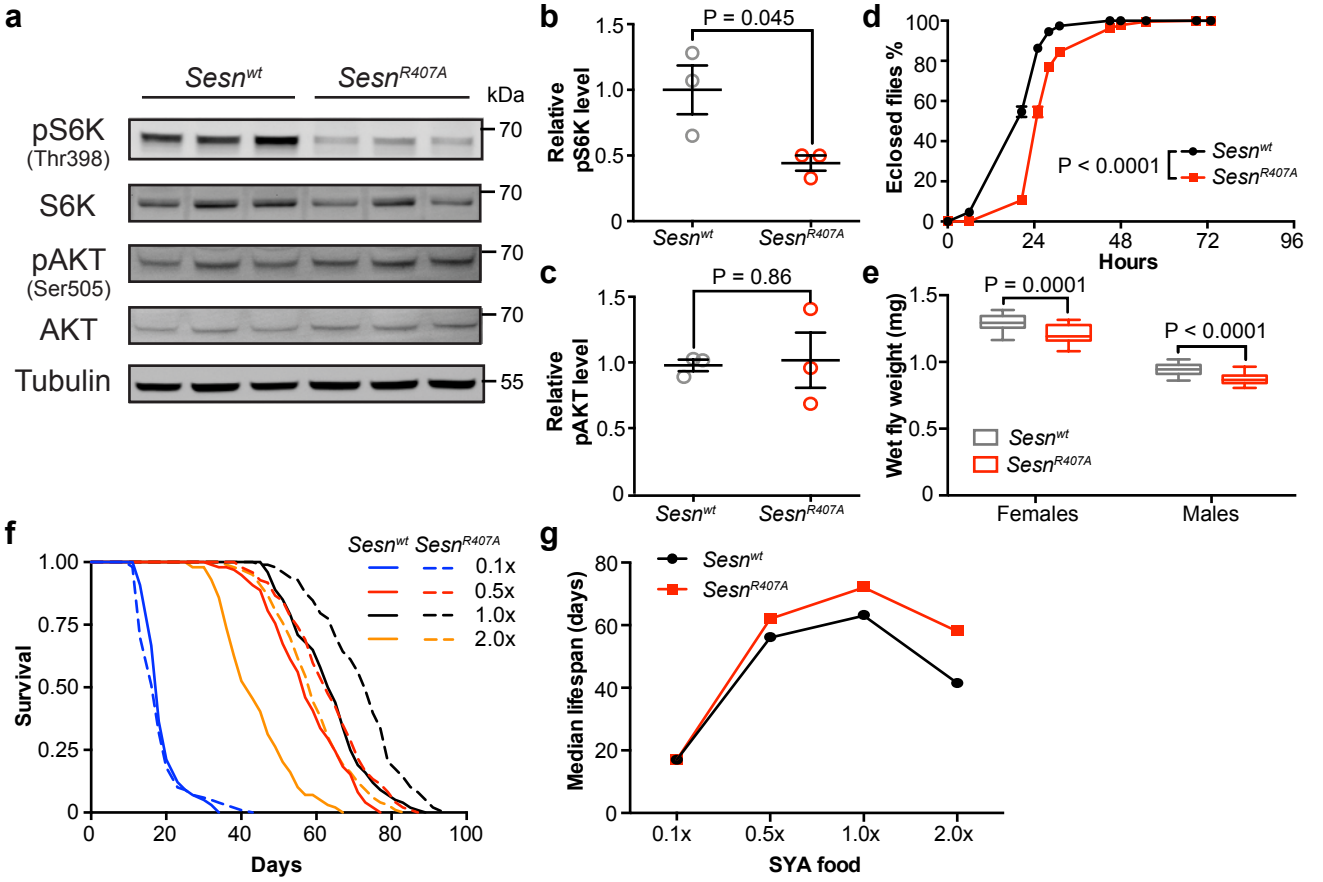
a
Sesn^wt
Sesn^R407A
kDa
pS6K
(Thr398)
S6K
pAKT
(Ser505)
AKT
Tubulin
70
70
70
70
55
b
Relative pS6K level
P = 0.045
Sesn^wt
Sesn^R407A
c
Relative pAKT level
P = 0.86
Sesn^wt
Sesn^R407A
d
Eclosed flies %
P < 0.0001
Sesn^wt
Sesn^R407A
Hours
e
Wet fly weight (mg)
P = 0.0001
P < 0.0001
Sesn^wt
Sesn^R407A
Females
Males
f
Survival
Days
Sesn^wt Sesn^R407A
0.1x
0.5x
1.0x
2.0x
g
Median lifespan (days)
Sesn^wt
Sesn^R407A
SYA food

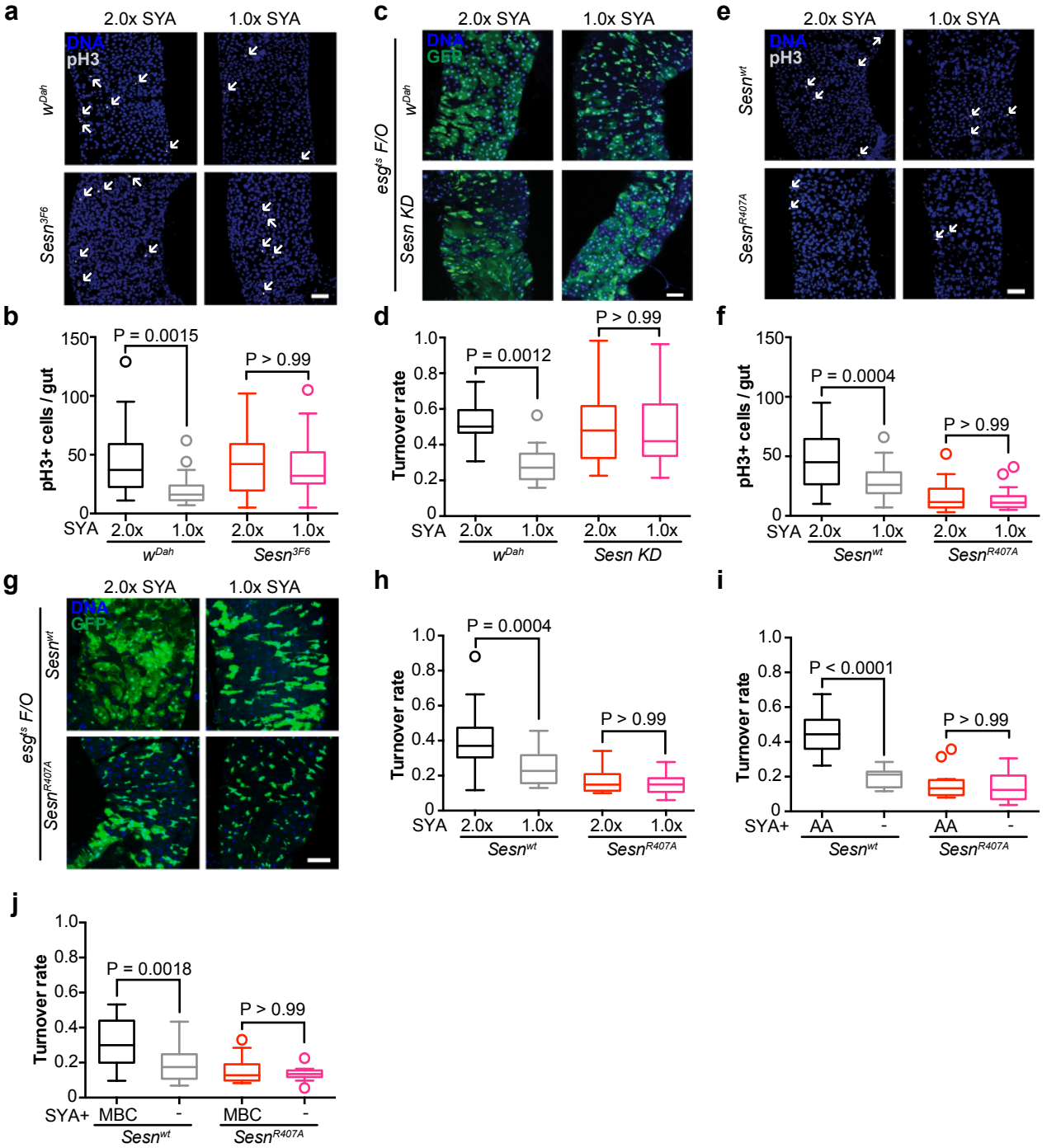
a
2.0x SYA
1.0x SYA
DNA
pH3
w^{Dah}
$Sesn^{3F6}$
b
pH3+ cells / gut
P = 0.0015
P > 0.99
SYA 2.0x 1.0x 2.0x 1.0x
w^{Dah}
$Sesn^{3F6}$
c
DNA
GFP
esg^{ts} F/O
w^{Dah}
Sesn KD
d
Turnover rate
P = 0.0012
P > 0.99
SYA 2.0x 1.0x 2.0x 1.0x
w^{Dah}
Sesn KD
e
DNA
pH3
$Sesn^{wt}$
$Sesn^{R407A}$
f
pH3+ cells / gut
P = 0.0004
P > 0.99
SYA 2.0x 1.0x 2.0x 1.0x
$Sesn^{wt}$
$Sesn^{R407A}$
g
2.0x SYA
1.0x SYA
DNA
GFP
esg^{ts} F/O
$Sesn^{wt}$
$Sesn^{R407A}$
h
Turnover rate
P = 0.0004
P > 0.99
SYA 2.0x 1.0x 2.0x 1.0x
$Sesn^{wt}$
$Sesn^{R407A}$
i
Turnover rate
P < 0.0001
P > 0.99
SYA+ AA - AA -
$Sesn^{wt}$
$Sesn^{R407A}$
j
Turnover rate
P = 0.0018
P > 0.99
SYA+ MBC - MBC -
$Sesn^{wt}$
$Sesn^{R407A}$

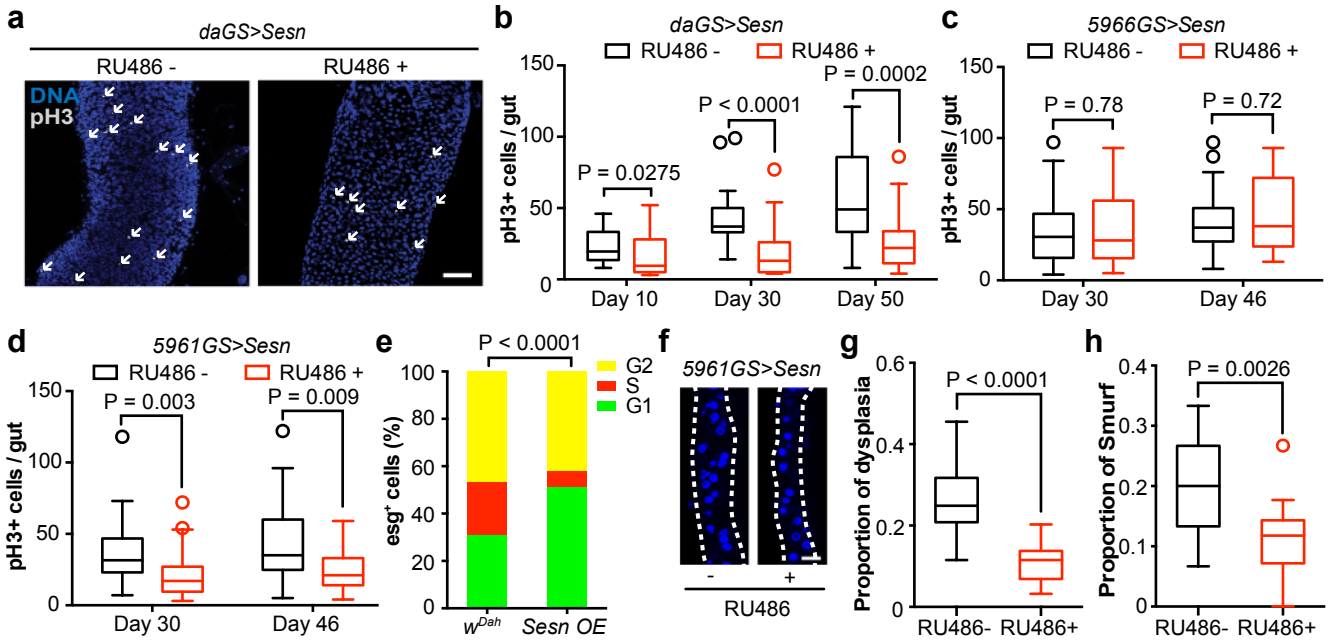
a
daGS>Sesn
RU486 -
RU486 +
DNA
pH3
b
daGS>Sesn
RU486 -
RU486 +
pH3+ cells / gut
P = 0.0275
P < 0.0001
P = 0.0002
Day 10
Day 30
Day 50
c
5966GS>Sesn
RU486 -
RU486 +
pH3+ cells / gut
P = 0.78
P = 0.72
Day 30
Day 46
d
5961GS>Sesn
RU486 -
RU486 +
pH3+ cells / gut
P = 0.003
P = 0.009
Day 30
Day 46
e
P < 0.0001
esg+ cells (%)
G2
S
G1
wDah
Sesn OE
f
5961GS>Sesn
RU486
g
Proportion of dysplasia
P < 0.0001
RU486-
RU486+
h
Proportion of Smurf
P = 0.0026
RU486-
RU486+

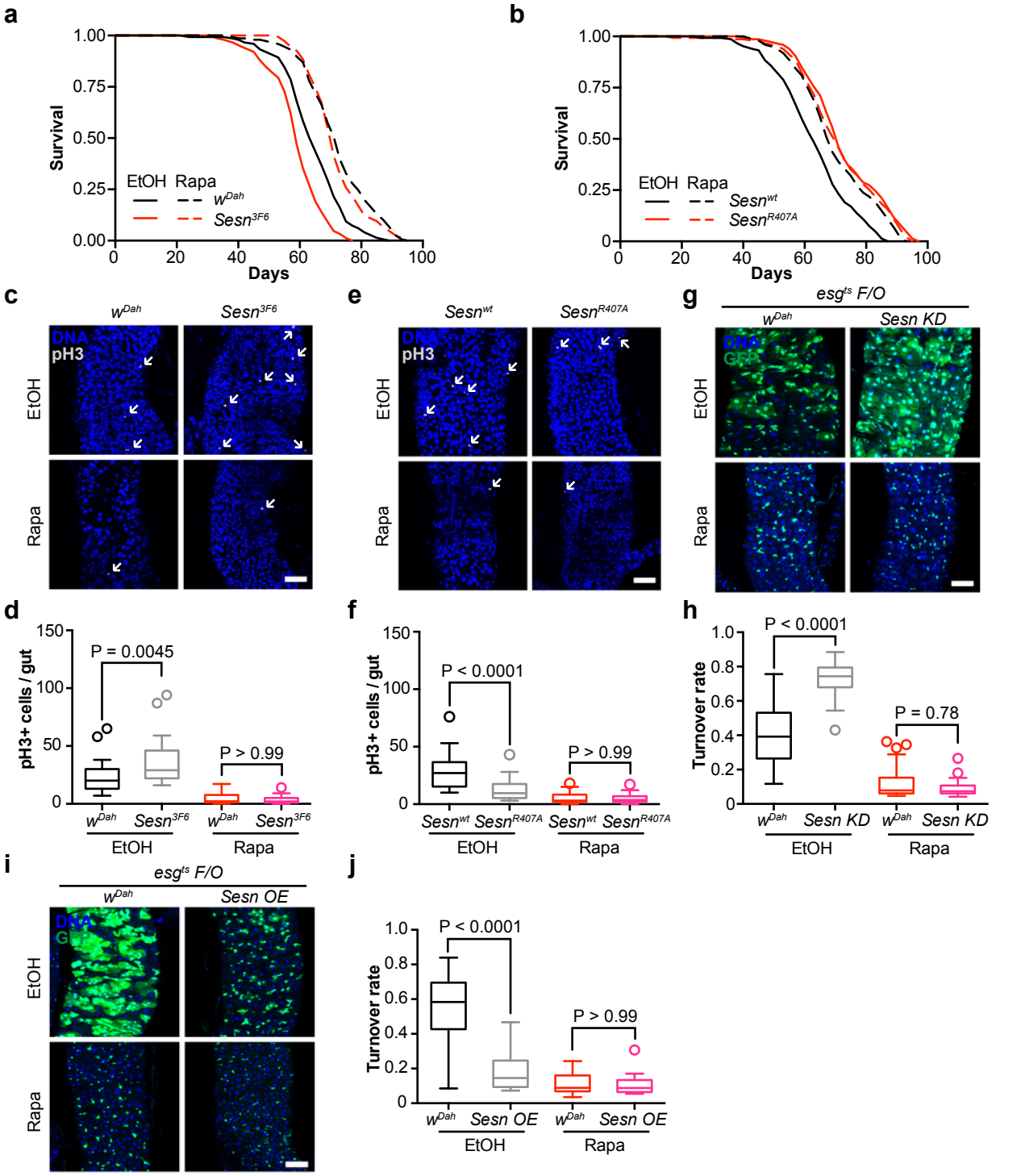
a
Survival
1.00
0.75
0.50
0.25
0.00
0
20
40
60
80
100
Days
EtOH Rapa
wDah
Sesn3F6
b
Survival
1.00
0.75
0.50
0.25
0
0
20
40
60
80
100
Days
EtOH Rapa
Sesnwt
SesnR407A
c
wDah
Sesn3F6
DNA
pH3
EtOH
Rapa
e
Sesnwt
SesnR407A
DNA
pH3
EtOH
Rapa
g
esgts F/O
wDah
Sesn KD
DNA
GFP
EtOH
Rapa
d
pH3+ cells / gut
150
100
50
0
P = 0.0045
P > 0.99
wDah
Sesn3F6
wDah
Sesn3F6
EtOH
Rapa
f
pH3+ cells / gut
150
100
50
0
P < 0.0001
P > 0.99
Sesnwt
SesnR407A
Sesnwt
SesnR407A
EtOH
Rapa
h
Turnover rate
1.0
0.8
0.6
0.4
0.2
0
P < 0.0001
P = 0.78
wDah
Sesn KD
wDah
Sesn KD
EtOH
Rapa
i
esgts F/O
wDah
Sesn OE
DNA
GFP
EtOH
Rapa
j
Turnover rate
1.0
0.8
0.6
0.4
0.2
0
P < 0.0001
P > 0.99
wDah
Sesn OE
wDah
Sesn OE
EtOH
Rapa

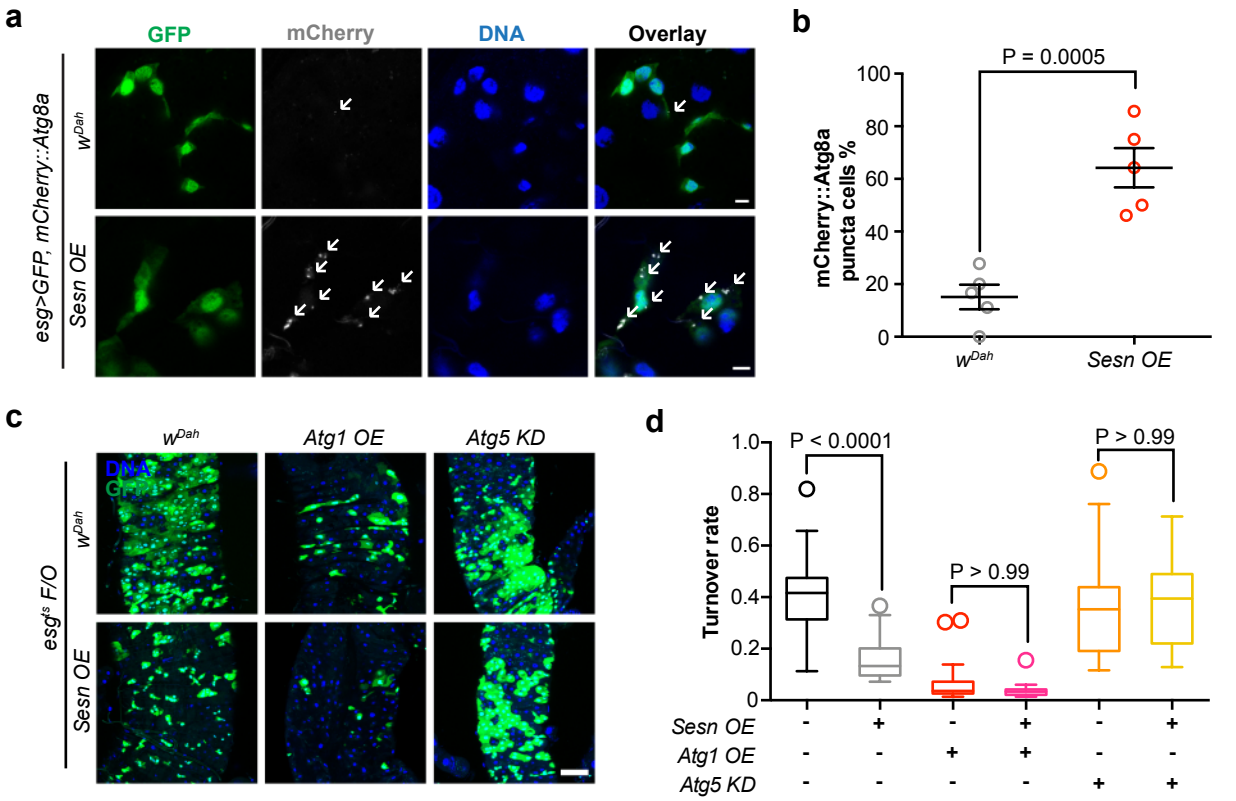
a
GFP
mCherry
DNA
Overlay
esg>GFP, mCherry::Atg8a
w^Dah
Sesn OE
b
P = 0.0005
mCherry::Atg8a puncta cells %
100
80
60
40
20
0
w^Dah
Sesn OE
c
w^Dah
Atg1 OE
Atg5 KD
esg^ts F/O
DNA
GFP
w^Dah
Sesn OE
d
P < 0.0001
P > 0.99
P > 0.99
Turnover rate
1.0
0.8
0.6
0.4
0.2
0
Sesn OE
Atg1 OE
Atg5 KD

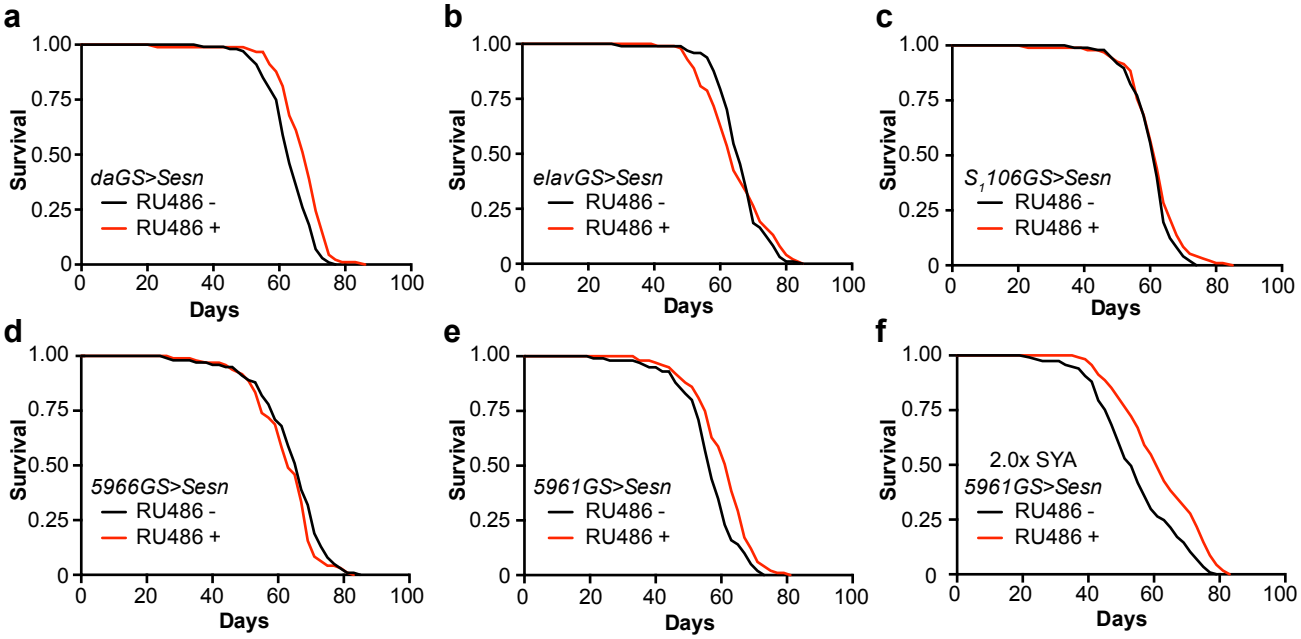
a
b
c
d
e
f
Survival
Days
1.00
0.75
0.50
0.25
0
0
20
40
60
80
100
daGS>Sesn
elavGS>Sesn
S1106GS>Sesn
5966GS>Sesn
5961GS>Sesn
2.0x SYA
5961GS>Sesn
RU486 -
RU486 +

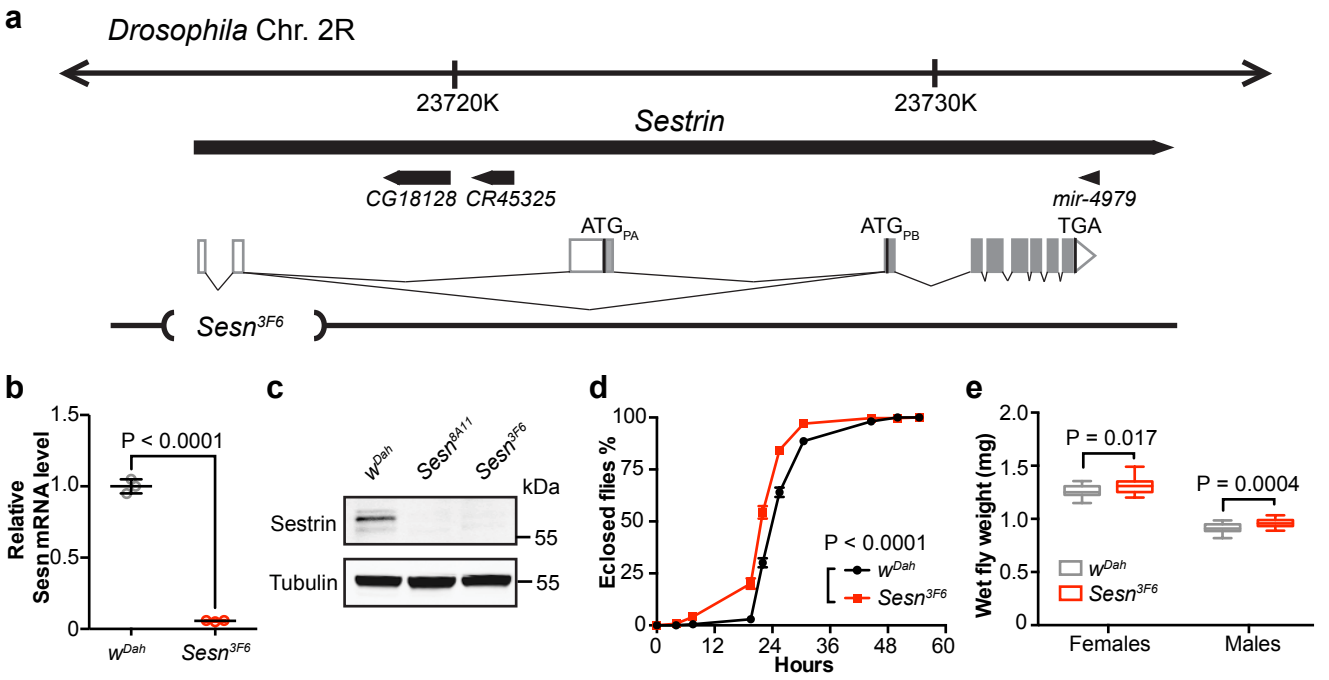
a
Drosophila Chr. 2R
23720K
23730K
Sestrin
CG18128
CR45325
mir-4979
ATG PA
ATG PB
TGA
Sesn 3F6
b
Relative Sesn mRNA level
P < 0.0001
w Dah
Sesn 3F6
c
w Dah
Sesn 8A11
Sesn 3F6
kDa
Sestrin
Tubulin
55
55
d
Eclosed flies %
P < 0.0001
w Dah
Sesn 3F6
Hours
e
Wet fly weight (mg)
P = 0.017
P = 0.0004
w Dah
Sesn 3F6
Females
Males

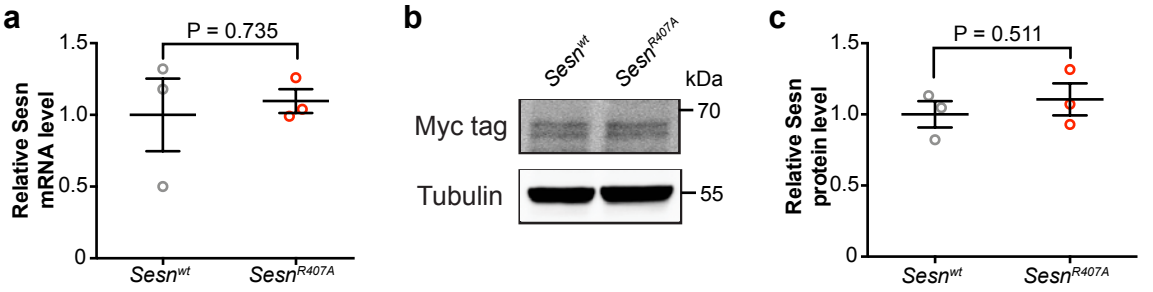
a
P = 0.735
Relative Sesn mRNA level
1.5
1.0
0.5
0
Sesn^wt
Sesn^R407A
b
Sesn^wt
Sesn^R407A
kDa
Myc tag
70
Tubulin
55
c
P = 0.511
Relative Sesn protein level
1.5
1.0
0.5
0
Sesn^wt
Sesn^R407A

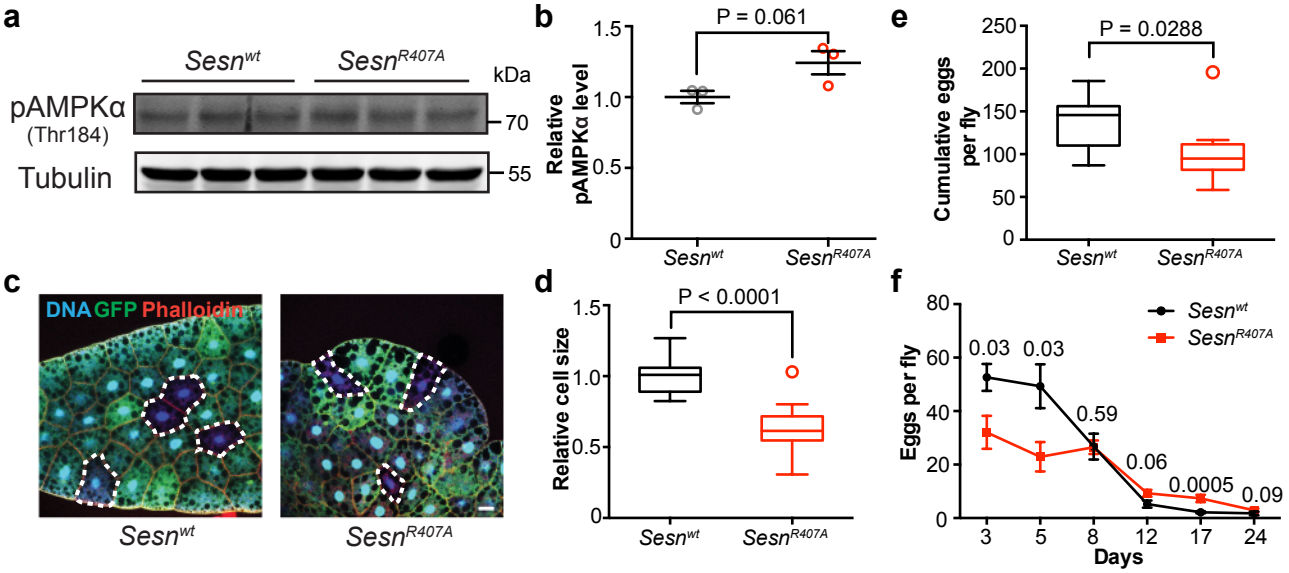
a
Sesn^wt
Sesn^R407A
kDa
pAMPKα
(Thr184)
70
Tubulin
55
b
P = 0.061
Relative pAMPKα level
1.5
1.0
0.5
0
Sesn^wt
Sesn^R407A
e
P = 0.0288
Cumulative eggs per fly
250
200
150
100
50
0
Sesn^wt
Sesn^R407A
c
DNA GFP Phalloidin
Sesn^wt
Sesn^R407A
d
P < 0.0001
Relative cell size
1.5
1.0
0.5
0
Sesn^wt
Sesn^R407A
f
Sesn^wt
Sesn^R407A
Eggs per fly
80
60
40
20
0
0.03
0.03
0.59
0.06
0.0005
0.09
3
5
8
12
17
24
Days

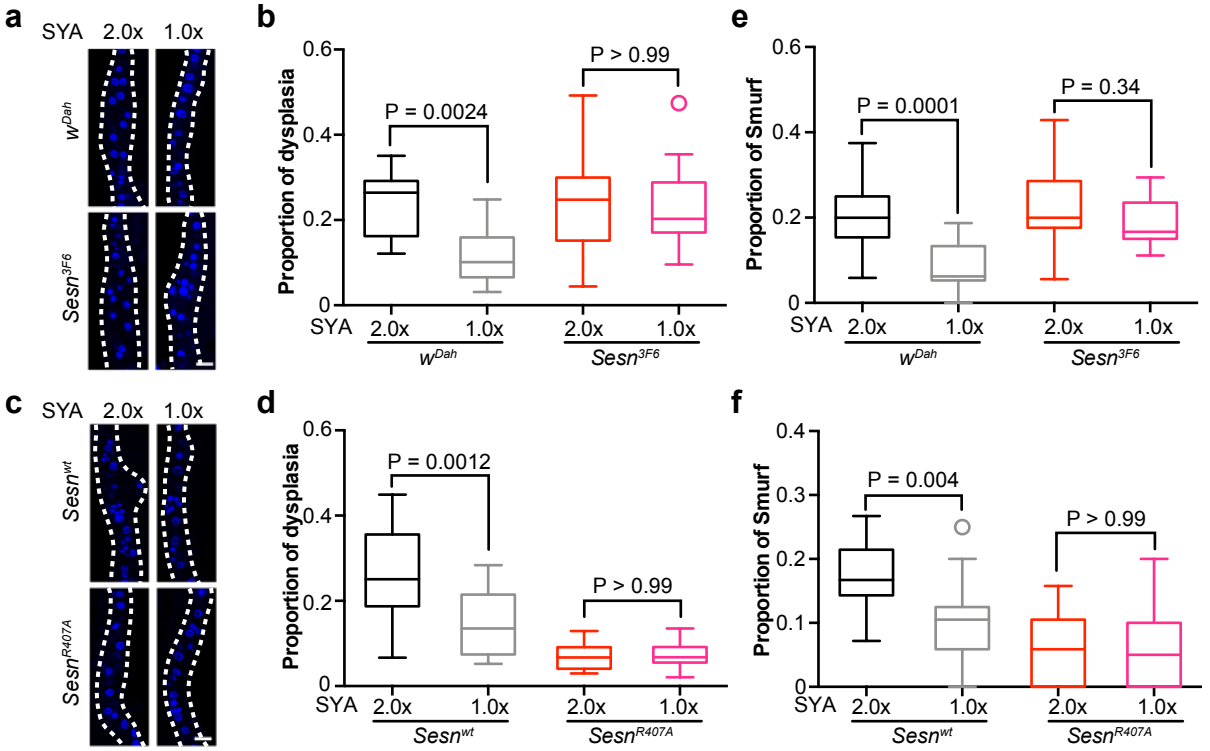
a
SYA 2.0x 1.0x
w^{Dah}
$Sesn^{3F6}$
b
Proportion of dysplasia
0.6
0.4
0.2
0
P = 0.0024
P > 0.99
SYA 2.0x 1.0x 2.0x 1.0x
w^{Dah}
$Sesn^{3F6}$
e
Proportion of Smurf
0.6
0.4
0.2
0
P = 0.0001
P = 0.34
SYA 2.0x 1.0x 2.0x 1.0x
w^{Dah}
$Sesn^{3F6}$
c
SYA 2.0x 1.0x
$Sesn^{wt}$
$Sesn^{R407A}$
d
Proportion of dysplasia
0.6
0.4
0.2
0
P = 0.0012
P > 0.99
SYA 2.0x 1.0x 2.0x 1.0x
$Sesn^{wt}$
$Sesn^{R407A}$
f
Proportion of Smurf
0.4
0.3
0.2
0.1
0
P = 0.004
P > 0.99
SYA 2.0x 1.0x 2.0x 1.0x
$Sesn^{wt}$
$Sesn^{R407A}$

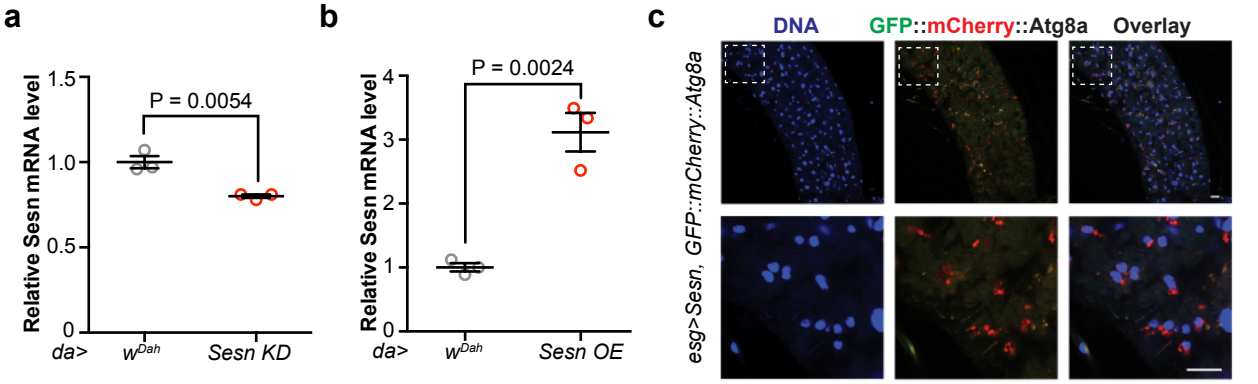
a
Relative Sesn mRNA level
1.5
1.0
0.5
0
P = 0.0054
da>
w^Dah
Sesn KD
b
Relative Sesn mRNA level
4
3
2
1
0
P = 0.0024
da>
w^Dah
Sesn OE
c
DNA
GFP::mCherry::Atg8a
Overlay
esg>Sesn, GFP::mCherry::Atg8a

Supplementary Table 1

Supplementary Table 1: Fly strains used in this study.

Fly Strains	Source	Identifier
w^{Dah}	This lab	
w; $Sesn^{3F6}$	J.H. Lee	
w; $Sesn^{8A11}$	J.H. Lee	
w^{Dah}; $Sesn^{wt}$	This paper	
w^{Dah}; $Sesn^{R407A}$	This paper	
w^{Dah}; UAS-Sesn	This paper	
w^{1118}; UAS-Sesn RNAi	VDRC	ID 38481
w^{Dah}; UAS-Atg1	This lab	GS10797
w^{Dah}; UAS-Atg5 RNAi	This lab	
w; neoFRT42D	BDSC	BL 1802
w^{1118}; neoFRT42D, Ubi-GFP	BDSC	BL 5626
w; esg-Gal4, tubGal80^{ts}, UAS-GFP; UAS-flp, Act>CD2>Gal4	B. Edgar	
w^{1118}; UAS-GFP-E2F1, UAS-mRFP1-NLS-CycB / CyO, wg-lacZ; MKRS / TM6B	B. Edgar	
yw,hsFlp; UAS-mCherry-Atg8a	G. Juhasz	
yw; UAS-GFP-mCherry-Atg8a	BDSC	BL 37749
w^{Dah}; daGS	This lab	
w^{Dah}; 5966GS	This lab	
w^{Dah}; 5961GS	This lab	
w^{Dah}; elavGS	This lab	
w^{Dah}; $S_1$106GS	This lab	

Supplementary Table 2

Supplementary Table 2: Fly genotypes in each figure.

Figure	Genotype
Fig. 1	Control: w^{Dah} Mutant: w^{Dah}; $Sesn^{3F6}$
Fig. 2	(2f-i), Control: w^{Dah}; $Sesn^{wt}$ Mutant: w^{Dah}; $Sesn^{R407A}$
Fig. 3	Control: w^{Dah}; $Sesn^{wt}$ Mutant: w^{Dah}; $Sesn^{R407A}$
Fig. 4	(4a,b), Control: w^{Dah} Mutant: w^{Dah}; $Sesn^{3F6}$
	(4c,d), w^{Dah}: *w; esg-Gal4, tubGal80^{ts}, UAS-GFP / +; UAS-flp,Act>CD2>Gal4 / +* *Sesn KD*: *w*; *esg-Gal4, tubGal80^{ts}, UAS-GFP / +; UAS-flp,Act>CD2>Gal4 / UAS-Sesn RNAi*
	(4e,f), Control: w^{Dah}; $Sesn^{wt}$ Mutant: w^{Dah}; $Sesn^{R407A}$
	(4g-j), $Sesn^{wt}$: *w; esg-Gal4, tubGal80^{ts}, UAS-GFP, Sesn^{wt} / Sesn^{wt}; UAS-flp,Act>CD2>Gal4 / +* $Sesn^{R407A}$: *w*; *esg-Gal4, tubGal80^{ts}, UAS-GFP, Sesn^{R407A} / Sesn^{R407A}; UAS-flp,Act>CD2>Gal4 / +*
Fig. 5	(5a,b), w^{Dah}; *daGS / +*; *UAS-Sesn / +*
	(5c), w^{Dah}; *5966GS / +*; *UAS-Sesn / +*
	(5d), w^{Dah}; *5961GS / +*; *UAS-Sesn / +*
	(5e), w^{Dah}: *w; esg-Gal4 / UAS-GFP-E2F1, UAS-mRFP1-NLS-CycB; +* *Sesn OE*: *w*; *esg-Gal4 / UAS-GFP-E2F1, UAS-mRFP1-NLS-CycB; UAS-Sesn / +*
	(5f-h), w^{Dah}; *5961GS / +*; *UAS-Sesn / +*
Fig. 6	(6a,c,d), Control: w^{Dah} Mutant: w^{Dah}; $Sesn^{3F6}$
	(6b,e,f), Control: w^{Dah}; $Sesn^{wt}$ Mutant: w^{Dah}; $Sesn^{R407A}$
	(6g,h), w^{Dah}: *w; esg-Gal4, tubGal80^{ts}, UAS-GFP / +; UAS-flp,Act>CD2>Gal4 / +* *Sesn KD*: *w*; *esg-Gal4, tubGal80^{ts}, UAS-GFP / +; UAS-flp,Act>CD2>Gal4 / UAS-Sesn RNAi*
	(6i,j), w^{Dah}: *w; esg-Gal4, tubGal80^{ts}, UAS-GFP / +; UAS-flp,Act>CD2>Gal4 / +* *Sesn OE*: *w*; *esg-Gal4, tubGal80^{ts}, UAS-GFP / +; UAS-flp,Act>CD2>Gal4 / UAS-Sesn*
Fig. 7	(7a,b), w^{Dah}: w^{Dah}*; esg-Gal4, UAS-GFP / UAS-mCherry-Atg8a; +* *Sesn OE*: w^{Dah}; *esg-Gal4, UAS-GFP / UAS-mCherry-Atg8a; UAS-Sesn / +*
	(7c,d), w^{Dah}: *w; esg-Gal4, tubGal80^{ts}, UAS-GFP / +; UAS-flp,Act>CD2>Gal4 / +* *Sesn OE*: *w*; *esg-Gal4, tubGal80^{ts}, UAS-GFP / +; UAS-flp,Act>CD2>Gal4 / UAS-Sesn* *Atg1 OE*: *w*; *esg-Gal4, tubGal80^{ts}, UAS-GFP / +; UAS-flp,Act>CD2>Gal4 / UAS-Atg1* *Sesn OE, Atg1 OE*: *w*; *esg-Gal4, tubGal80^{ts}, UAS-GFP / +; UAS-flp,Act>CD2>Gal4 / UAS-Atg1*, *UAS-Sesn* *Atg5 KD: w, Atg5 RNAi; esg-Gal4, tubGal80^{ts}, UAS-GFP / +; UAS-flp,Act>CD2>Gal4 / +* *Sesn OE*, *Atg5 KD: w, Atg5 RNAi; esg-Gal4, tubGal80^{ts}, UAS-GFP / +; UAS-flp,Act>CD2>Gal4 / UAS-Sesn*
Fig. 8	(8a), w^{Dah}; *daGS / +*; *UAS-Sesn / +*
	(8b), w^{Dah}; *+*; *elavGS / UAS-Sesn*
	(8c), w^{Dah}; *$S_1$106GS / +*; *UAS-Sesn / +*
	(8d), w^{Dah}; *5966GS / +*; *UAS-Sesn / +*
	(8e,f), w^{Dah}; *5961GS / +*; *UAS-Sesn / +*
Supplementary Fig. 1	Control: w^{Dah} Mutant: w^{Dah}; $Sesn^{3F6}$
Supplementary Fig. 2	Control: w^{Dah}; $Sesn^{wt}$ Mutant: w^{Dah}; $Sesn^{R407A}$

Supplementary Fig. 3	(3a,b), Control: w^{Dah}; $Sesn^{wt}$ Mutant: w^{Dah}; $Sesn^{R407A}$
	(3c,d), $Sesn^{wt}$: *yw, hsFlp; neoFRT42D, $Sesn^{wt}$ / neoFRT42D, Ubi-GFP* $Sesn^{R407A}$: *yw, hsFlp; neoFRT42D, $Sesn^{R407A}$ / neoFRT42D, Ubi-GFP*
	(3e,f), Control: w^{Dah}; $Sesn^{wt}$ Mutant: w^{Dah}; $Sesn^{R407A}$
Supplementary Fig. 4	(4a,b,e), Control: w^{Dah} Mutant: w^{Dah}; $Sesn^{3F6}$
	(4c,d,f), Control: w^{Dah}; $Sesn^{wt}$ Mutant: w^{Dah}; $Sesn^{R407A}$
Supplementary Fig. 5	(5a), w^{Dah}: w^{Dah}*; +; da-Gal4 / +* *Sesn KD*: w^{Dah}; *+; da-Gal4 / UAS-Sesn RNAi*
	(5b), w^{Dah}: w^{Dah}*; +; da-Gal4 / +* *Sesn OE*: w^{Dah}; *+; da-Gal4 / UAS-Sesn*
	(5c), w^{Dah}; *esg-Gal4 / UAS-GFP-mCherry-Atg8a; UAS-Sesn / +*

Supplementary Table 3

Supplementary Table 3: Oligos, related to Methods.

Name	Sequence (5' to 3')	Application
Sesn fwd	TAACCGCTCGAGATGTACTACGCCGTCGATTACTAC	Sesn cDNA cloning
Sesn rev	TACTAGTCTAGATCAAGTCATATAGCGCATTATCTC	Sesn cDNA cloning
qSesn fwd	CGAAGTGAACCAGCTCCTG	Sesn qPCR
qSesn rev	CAGCTCGACCAGCACACTAT	Sesn qPCR
qRpl32 fwd	ATATGCTAAGCTGTCGCACAAATGG	Rpl32 qPCR
qRpl32 rev	GATCCGTAACCGATGTTGGGCA	Rpl32 qPCR
HA fwd	TAACCGGAATTCATGTACTACGCCGTCGATTACTAC	Sesn and Sesn^{R407A} cloning to pcDNA3
HA rev	TACTAGGCGGCCGCTCAAGTCATATAGCGCATTATCTCGC	Sesn and Sesn^{R407A} cloning to pcDNA3
WDR24 fwd	TAACCGGAATTCATGCCCGATTCCGTGGAGGAC	WDR24 cDNA cloning
WDR24 rev	TACTAGGCGGCCGCTCATGAGTACGCGCAAAGGTG	WDR24 cDNA cloning
Sesn gRNA fwd	TATATAGGAAAGATATCCGGGTGAACTTCGAAATATATTT AATTTACCAGTTTTAGAGCTAGAAATAGCAAG	Sesn gRNA cloning
Sesn gRNA rev	ATTTTAACTTGCTATTTCTAGCTCTAAAACATTATCTCTCC ATCAAAAGCGACGTTAAATTGAAAATAGGTC	Sesn gRNA cloning
pOT CDR fwd	AATCGCGGATCCCATTAATGAATCGGCTGCAG	Sesn donor construct: R407 region cloning
pOT CDR rev	AATCGCGCTAGCGTGTCACCTAAATCGTATGTGTATG	Sesn donor construct: R407 region cloning
Sesn CDR fwd	AATCGCGCTAGCCCCCTCCTCATTCACTTGC	Sesn donor construct: R407 region cloning
Sesn CDR rev	AATCGCGGATCCAGTCATATAGCGCATTATCTCGC	Sesn donor construct: R407 region cloning
Sesn R407A fwd	GGACACGTCCAAGTTCGCGCGGGCCATTTG	Sesn R407A mutagenesis
Sesn R407A rev	CAAATGGCCCGCGCGAACTTGGACGTGTCC	Sesn R407A mutagenesis
pOT donor fwd	AATCGCGGTACCACACTAGAATTCCATTAATGAATCGGCT GCAG	Sesn donor construct: vector region cloning
pOT donor rev	AATCGCGGATCCACACATGCTAGCACACTACTCGAGGTG TCACCTAAATCGTATGTG	Sesn donor construct: vector region cloning
Myc tag fwd	AATCGCGGATCCGGATCTGAGCAAAAGCTCATTTCTGAA GAGGACTTGTGATCTCATTAAGTGAATAAACATA	Sesn donor construct: tag cloning
Myc tag rev	AATCGCGGTACCATCTCTCCATCAAAAGCTCG	Sesn donor construct: tag cloning
Sesn LR fwd	AATCGCCTCGAGGTTGGATTGCGATGTGAGTG	Sesn donor construct: left arm cloning
Sesn LR rev	AATCGCGCTAGCTAAATTAAATATATTTCTGTTTAGAACA GTTCAGTG	Sesn donor construct: left arm cloning
Sesn RR fwd	AATCGCGGTACCTATAAATGTCTATTTTGATAGTATTTAA ATCAAC	Sesn donor construct: right arm cloning
Sesn RR rev	AATCGCGAATTCTTGCATTGCCATCTTCAA	Sesn donor construct: right arm cloning

Supplementary Table 4

Supplementary Table 4: Details of lifespan assays, related to Fig. 1, 3, 6.

Genotype	Group*	Treatment	Dead	Censored	Median	P value
w^{Dah}	1	0.1x SYA	98	2	18.5	0.79
$Sesn^{3F6}$	1	0.1x SYA	100	0	21	
w^{Dah}	1	0.5x SYA	97	3	65	$5.9x10^{-7}$
$Sesn^{3F6}$	1	0.5x SYA	98	2	59	
w^{Dah}	1	1.0x SYA	99	1	60.5	$6.5x10^{-6}$
$Sesn^{3F6}$	1	1.0x SYA	98	2	53.5	
w^{Dah}	1	2.0x SYA	99	1	42	0.14
$Sesn^{3F6}$	1	2.0x SYA	99	1	39.5	
w^{Dah}	3	0.1x SYA	100	0	17	0.10
$Sesn^{3F6}$	3	0.1x SYA	99	1	19	
w^{Dah}	3	0.5x SYA	99	1	56	$4.4x10^{-5}$
$Sesn^{3F6}$	3	0.5x SYA	98	2	50	
w^{Dah}	3	1.0x SYA	98	2	64	$4.8x10^{-14}$
$Sesn^{3F6}$	3	1.0x SYA	98	2	56	
w^{Dah}	3	2.0x SYA	100	0	40	0.18
$Sesn^{3F6}$	3	2.0x SYA	98	2	39	
$Sesn^{wt}$	2	1.0x SYA	199	1	57	$1.1x10^{-28}$
$Sesn^{R407A}$	2	1.0x SYA	194	6	67.5	
$Sesn^{wt}$	3	0.1x SYA	99	1	17	0.34
$Sesn^{R407A}$	3	0.1x SYA	100	0	17	
$Sesn^{wt}$	3	0.5x SYA	98	2	56	$9.8x10^{-5}$
$Sesn^{R407A}$	3	0.5x SYA	97	3	62	
$Sesn^{wt}$	3	1.0x SYA	100	0	63	$9.0x10^{-8}$
$Sesn^{R407A}$	3	1.0x SYA	98	2	72	
$Sesn^{wt}$	3	2.0x SYA	99	1	41.5	$1.8x10^{-20}$
$Sesn^{R407A}$	3	2.0x SYA	99	1	58	
w^{Dah}	4	1.0x SYA EtOH	149	1	64	$6.4x10^{-11}$
w^{Dah}	4	1.0x SYA Rapa	146	4	72	
$Sesn^{3F6}$	4	1.0x SYA EtOH	150	0	58	$2.1x10^{-29}$
$Sesn^{3F6}$	4	1.0x SYA Rapa	147	3	70	
$Sesn^{wt}$	4	1.0x SYA EtOH	147	3	62	$1.0x10^{-6}$
$Sesn^{wt}$	4	1.0x SYA Rapa	147	3	68	
$Sesn^{R407A}$	4	1.0x SYA EtOH	146	4	70	0.37
$Sesn^{R407A}$	4	1.0x SYA Rapa	147	3	70	

*: Group numbers indicate experiments run in parallel.

Supplementary Table 5

Supplementary Table 5: Details of lifespan assays, related to Fig. 8.

Genotype	Group*	Treatment	Dead	Censored	Median	P value
daGS	2	1.0x SYA RU486-	98	2	68	0.20
	2	1.0x SYA RU486+	100	0	66	
UAS-Sesn	2	1.0x SYA RU486-	100	0	64	0.75
	2	1.0x SYA RU486+	98	2	65	
UAS-Sesn	4	1.0x SYA RU486-	98	2	71	0.21
	4	1.0x SYA RU486+	100	0	67	
daGS>Sesn	2	1.0x SYA RU486-	100	0	63	$7.7x10^{-4}$
	2	1.0x SYA RU486+	95	5	66	
daGS>Sesn	1	1.0x SYA RU486-	99	1	63	$1.1x10^{-4}$
	1	1.0x SYA RU486+	100	0	67	
daGS>Sesn	2	1.0x SYA RU486-	100	0	62	$2.2x10^{-5}$
	2	1.0x SYA RU486+	90	10	68	
elavGS>Sesn	1	1.0x SYA RU486-	97	3	65	0.82
	1	1.0x SYA RU486+	99	1	63	
$S_1$106>Sesn	1	1.0x SYA RU486-	97	3	61	0.15
	1	1.0x SYA RU486+	95	5	61	
5966GS>Sesn	3	1.0x SYA RU486-	100	0	66	0.09
	3	1.0x SYA RU486+	96	4	62	
5961GS>Sesn	3	1.0x SYA RU486-	100	0	56	$4.2\ x10^{-4}$
	3	1.0x SYA RU486+	99	1	62	
5961GS>Sesn	4	1.0x SYA RU486-	98	2	59	$2.1x10^{-4}$
	4	1.0x SYA RU486+	95	5	63	
5961GS	4	1.0x SYA RU486-	96	4	68	0.32
	4	1.0x SYA RU486+	100	0	67	
5961GS	5	2.0x SYA RU486-	117	3	54	0.97
	5	2.0x SYA RU486+	118	2	52	
UAS-Sesn	5	2.0x SYA RU486-	118	2	52	0.09
	5	2.0x SYA RU486+	117	3	48	
5961GS>Sesn	5	2.0x SYA RU486-	117	3	52	$5.4x10^{-6}$
	5	2.0x SYA RU486+	115	5	60	

*: Group numbers indicate experiments run in parallel.

Supplementary Table 6

Supplementary Table 6: Amino acid levels in *Drosophila* S2R+ cells.

Amino acids	Conc. (mM)	Amino acids	Conc. (mM)
Leu	3.9±0.2	Ala	37.0±2.7
Ile	2.8±0.3	Asn	0.75±0.07
Val	6.7±0.3	Asp	10.6±1.0
Met	3.1±0.2	Cys	0.20±0.03
Arg	5.8±0.4	Glu	20.7±1.6
Phe	0.39±0.05	Gln	17.2±0.7
His	6.4±0.4	Gly	13.2±1.5
Lys	5.3±0.3	Pro	18.0±0.9
Thr	7.1±0.5	Ser	6.6±0.5
Trp	1.6±0.2	Tyr	1.8±0.1

Supplementary Table 7

Supplementary Table 7: Details of antibody sources, related to Methods.

Antibodies	Source	Identifier
Anti Sestrin rabbit polyclonal	J.H. Lee	N/A
Anti pH3 (S10) rabbit polyclonal	Cell signaling	Cat# 9701
Anti Myc (9B11) mouse monoclonal	Cell signaling	Cat# 2276
Anti Flag M2 mouse monoclonal	Sigma	Cat# F1804
Anti HA rabbit polyclonal	Sigma	Cat# H6908
Anti pS6K (T398) rabbit polyclonal	Cell signaling	Cat# 9209
Anti S6K rabbit polyclonal	This lab	N/A
Anti pAMPKα (T172) (40H9) rabbit monoclonal	Cell signaling	Cat# 2535
Anti pAKT (S505) rabbit polyclonal	Cell signaling	Cat# 4054
Anti AKT rabbit polyclonal	Cell signaling	Cat# 9272
Anti Tubulin (DM1A) mouse monoclonal	Sigma	Cat# T9026
Goat anti-rabbit IgG IRDye 680RD	LI-COR	Cat# 926-68071
Goat anti-mouse IgG IRDye 800CW	LI-COR	Cat# 926-32210
Goat anti-rabbit IgG (H+L), Alexa Fluor 594	Thermo Fisher Scientific	Cat# A11012